

2019-03-20

Abiotic degradation of highly branched isoprenoid alkenes and other lipids in the water column off East Antarctica

Rontani, JF

<http://hdl.handle.net/10026.1/13533>

10.1016/j.marchem.2019.02.004

Marine Chemistry

Elsevier

All content in PEARL is protected by copyright law. Author manuscripts are made available in accordance with publisher policies. Please cite only the published version using the details provided on the item record or document. In the absence of an open licence (e.g. Creative Commons), permissions for further reuse of content should be sought from the publisher or author.

Abiotic degradation of highly branched isoprenoid alkenes and other lipids in the water column off East Antarctica

Jean-François Rontani^{a,*}, Lukas Smik^b, Simon T. Belt^b, Frédéric Vaultier^a,

Linda Armbrecht^c, Amy Leventer^d, Leanne K. Armand^c

^a Aix Marseille Université, Université de Toulon, CNRS/INSU/IRD, Mediterranean Institute of Oceanography (MIO), UM 110, 13288 Marseille, France

^b Biogeochemistry Research Centre, School of Geography, Earth and Environmental Sciences, University of Plymouth, Drake Circus, Plymouth, Devon PL4 8AA, UK

^c Australian Centre for Ancient DNA, School of Biological Sciences, Faculty of Sciences, The University of Adelaide, Adelaide, South Australia, 5005, Australia

^d Department of Geology, Colgate University, Hamilton, NY 13346, USA

^e Research School of Earth Sciences, The Australian National University, Acton, Australian Capital Territory, 2601, Australia.

* Corresponding author. Tel.: +33-4-86-09-06-02; fax: +33-4-91-82-96-41. E-mail address: jean-francois.rontani@mio.osupytheas.fr (J.-F. Rontani)

Abstract. In some previous studies, the ratio between a di-unsaturated highly branched isoprenoid (HBI) lipid termed IPSO₂₅ and a structurally related tri-unsaturated counterpart (HBI III) (viz. IPSO₂₅/HBI III) has been used as a proxy measure of variable sea ice cover in the Antarctic owing to their production by certain sea ice algae and open water diatoms, respectively. To investigate this further, we quantified selected lipids and their photo- and autoxidation products in samples of suspended particulate matter (SPM) collected at different water depths in the polynya region west of the Dalton Iceberg Tongue (East Antarctica). The results obtained confirm the high efficiency of photo- and autoxidation processes in diatoms from the region. The systematic increase of the ratio IPSO₂₅/HBI III with water depth in the current samples appeared to be dependent on the sampling site and was due to both (i) a relatively higher contribution of ice algae to the deeper samples resulting from their increased aggregation and therefore higher sinking rate, or (ii) a stronger abiotic degradation of HBI III during settling through the water column. Analyses of samples taken from the water-sediment interface and some underlying near-surface sediments revealed a further increase of the ratio IPSO₂₅/HBI III, indicative of further differential oxidation of the more unsaturated HBI. Unfortunately, specific oxidation products of HBI III could not be detected in the strongly oxidized SPM and sediment samples, likely due to their lability towards further oxidation. In contrast, oxidation products of HBI III were detected in weakly oxidized samples of phytoplanktonic cells collected from Commonwealth Bay (also East Antarctica), thus providing more direct evidence for the involvement of photo- and/or autoxidation of HBI III in the region. This oxidative alteration of the ratio IPSO₂₅/HBI III between their source and sedimentary environments should be taken into account when using this parameter for palaeo sea ice reconstruction purposes in the Antarctic.

- 51 **Key words:** East Antarctica; Suspended particulate matter; Near-surface sediments; Lipids;
- 52 Photo- and autoxidation; Alteration of IPSO₂₅/HBI III ratio; Paleoceanographic implications.

1. Introduction

Sea ice plays a central role in the overall climate structure of the Polar Regions (Thomas, 2017). Amongst its various well known attributes, its high albedo (reflectivity) means that sea ice serves as an efficient regulator of incoming solar radiation to the surface oceans. Further, the physical structure of sea ice provides a physical barrier to the exchange of gas, heat and moisture between the polar oceans and the atmosphere. It is also an important contributor to near-surface stratification, bottom-water formation and ventilation, in particular (e.g. Dickson et al., 2007 and references therein). From a biogeochemical perspective, nutrient release during ice melt in spring, coupled with surface layer stratification and increasing light and temperature, often leads to intense open water phytoplankton production, especially along the retreating ice edge or the so-called marginal ice zone (MIZ) (Smith and Nelson 1986; Smith, 1987; Sakshaug et al., 2009; Perette et al., 2011).

Understanding the well documented abrupt changes in sea ice in the polar regions (Stroeve et al., 2012; Fetterer et al., 2016, Serreze et al., 2016; Walsh et al., 2017) requires more detailed knowledge of how it has changed in the past in response to other climatic drivers. A common approach to achieve this is through the analysis of so-called sea ice proxies present in marine sediment archives. The majority of these proxies possess some kind of biological origin, although there are others (e.g. de Vernal et al., 2013 and references therein). In the Antarctic, the identification of certain ice-associated diatoms in polar marine sediments has a long history of use for palaeo sea ice determinations (Armand et al., 2017). However, the growth habitat of the target species are normally more closely associated with the open waters of the MIZ rather than that of sea ice itself (Leventer, 1998; Leventer et al., 2008). On the other hand, those diatoms that bloom within the sea ice

host (i.e. the strictly sympagic community), are often under-represented in sedimentary records (Leventer, 2013).

Over the last decade or so, a number of diatom-derived lipid biomarkers have emerged as useful complementary sea ice proxies to the more traditional micropaleontological-based approaches. Thus a mono-unsaturated highly branched isoprenoid (HBI) termed IP₂₅ (Ice Proxy with 25 carbon atoms; Belt et al., 2007) has emerged as a useful proxy for seasonal Arctic sea ice (for reviews, see Belt and Muller, 2013; Belt, 2018), while a di-unsaturated structural homolog of IP₂₅ – sometimes referred to as HBI II (**1**; see appendix) – appears to be a suitable counterpart for the Antarctic. A recent source identification and the near ubiquity of the diene **1** in near-coastal sediments from around the Antarctic continent has led to its recent designation as IPSO₂₅ (Ice Proxy for the Southern Ocean with 25 carbon atoms; Belt et al., 2016) by analogy with IP₂₅. A further, tri-unsaturated HBI, often termed HBI III (**2**), is also showing potentially as a biomarker proxy indicator of the MIZ in both Polar Regions. Thus, enhanced concentrations of the triene **2** have been observed in surface sediments from the MIZ of the Barents Sea in the Arctic (Belt et al., 2015) and in surface waters of the MIZ in East Antarctica (Smik et al., 2016) and the Scotia Sea (Schmidt et al., 2018) shortly following sea ice melt. As a result, some palaeo sea records based on HBI II (hereafter referred to as IPSO₂₅) (**1**) and HBI III (**2**) for the Antarctic have appeared in recent years (Barbara et al., 2010,2013,2016; Denis et al., 2010; Collins et al., 2013; Etourneau et al., 2013; Campagne et al., 2015,2016). A general interpretation of greater sea ice extent for relatively high IPSO₂₅ (**1**) compared to HBI III (**2**), and more open water conditions for increased triene **2** concentrations has been applied. In some of these studies, variability in the ratio **1/2** has been used as a qualitative measure of changes to sea ice cover; however, this assumption has, as yet, not been validated through comparison of surface sediment biomarker data

with known overlying sea ice conditions in the same way as for IP₂₅ (and HBI III (2) in some cases) in the Arctic (see Belt, 2018 for a recent review). Nonetheless, such interpretations are consistent with the data reported by Smik et al. (2016) following analysis of IP_{SO₂₅} (1) and HBI III (2) in surface waters from regions of variable sea ice cover from East Antarctica, with highest concentrations found in the summer sea ice zone and MIZ, respectively. Similar findings have also been reported for surface water samples from the Scotia Sea (Schmidt et al., 2018). However, the extent to which the surface water distributions of IP_{SO₂₅} (1) and HBI III (2) are replicated in the underlying sediments for palaeo sea ice reconstruction purposes was not investigated in the initial study by Smik et al. (2016).

To provide further insight to this, here we carried out analysis of further water samples from the polynya region proximal to the Dalton Ice Tongue in East Antarctica with the primary aim of determining any variability of the ratio 1/2 with water depth, and to reconcile outcomes through the identification of pathway-specific oxidation products of common phytoplankton lipids as indicators of well-known degradation processes (i.e. bacterial degradation, photooxidation and autoxidation). Further evidence for the oxidation of such lipids was obtained through the analysis of near-surface sediment material collected from the main study region and from filtered phytoplankton samples collected from Commonwealth Bay (also East Antarctica).

2. Materials and methods

2.1. Sampling

Water samples were obtained as part of the NBP1402 cruise aboard the RVIB *Nathaniel B Palmer* in February–March 2014 as described previously (Smik et al., 2016;

see also NBP1402 Scientific Cruise Report, 2014, Sabrina Coast: Marine record of cryosphere–ocean dynamics (467 pages) for further details) (http://www.marinegeo.org/tools/search/data/field/NBPalmer/NBP1402/docs/NBP1402CruiseReport_Final.pdf). For the current study, we focused on those locations that had experienced seasonal sea ice cover within the polynya region west of the Dalton Iceberg Tongue (East Antarctica). At each of the 12 sampling sites (Fig. 1), surface (0–10 m), sub-surface (chlorophyll *a* maximum; ca. 25–60 m) and deep (ca. 500–1100 m) water samples were obtained from CTD rosettes. At the five stations where we carried out lipid degradation studies, the surface CTD samples had already been used for native lipid analyses so we used water obtained from the ship’s intake line (ca. <10 m); near-surface and deep water samples were obtained from the CTD rosettes as per the other stations. In each case, 1.5–3.0 l of sampled water was filtered onto 25 mm Whatman GF/F filters (as supplied), wrapped in aluminium foil and stored frozen (–80°C). Sample data are detailed in Supplementary Table 1. Megacoring was conducted using a Bowers and Connelly MegaCorer, with 12 10-cm diameter core tubes, for sampling an undisturbed sediment water interface. Surface water above the core tops and a layer of diatomaceous ‘fluff’ were pipetted off the top of the core tubes and stored frozen (–80°C). Sediment material from the cores was extruded at 0.5 to 2 cm intervals, depending on the core depth.

Three samples of phytoplankton cells (CB, AS607 and AS608) were collected in Commonwealth Bay (East Antarctica, 66°56S; 142°27E) during the IPEV-COCA2012 cruise in January 2012. Surface waters were sampled using a 25-µm ring net deployed from the R/V Astrolabe. Concentrated phytoplankton cell suspensions (ranging from 2.6 to 1.1 mg d.w. ml^{–1}) were stored frozen (–20 °C) prior to freeze drying and analysis.

2.2. Sample treatment

Lipids from all of the CTD samples, the waters above the sediment cores and the diatomaceous ‘fluff’ were extracted and analyzed as described previously by Smik et al. (2016). This treatment involved addition of internal standards (9-octyl-8-heptadecene for HBI quantification, 5 α -androstan-3 β -ol for Δ^5 -sterol quantification and nonadecanoic acid for fatty acid quantification), saponification (5% KOH (9:1 v/v MeOH/H₂O); 70 °C; 60 min) and separation of non-saponifiable (hexane 3x2 ml) and saponifiable fractions (+1 ml HCl; hexane (3x2 ml)). For sediments, ca. 1 g of freeze-dried material was extracted by sonication (dichloromethane/methanol; 2:1 v/v, 3x2 ml) to obtain a total organic extract (TOE). Subsequent purification of the unsaponifiable fraction/TOE by open column chromatography (SiO₂) afforded HBIs (elution with hexane; 5 column volumes) and sterols (elution with hexane-methyl acetate (4:1, v/v; 5 column volumes). In addition, saturated non-polar components of TOEs were removed using silver-ion chromatography (Belt et al., 2015).

Treatment of the filtered water samples from the five stations selected for lipid oxidation product analyses and phytoplankton material collected from Commonwealth Bay involved a different treatment. Following addition of MeOH (25 ml) and reduction with excess NaBH₄ (70 mg, 30 min) of labile hydroperoxides to alcohols, which are more amenable to analysis using gas chromatography–mass spectrometry (GC-MS), water (25 ml) and KOH (2.8 g) were added and the resulting mixture saponified by refluxing (2 h). After cooling, the mixture was acidified (HCl, 2 N) to pH 1 and extracted with dichloromethane (DCM; 3 x 20 ml). The combined DCM extracts were dried over anhydrous sodium sulfate, filtered and concentrated via rotary evaporation at 40°C to give total lipid extracts (TLEs).

A different treatment (Rontani et al., 2018) was employed to estimate the relative proportions of hydroperoxides and their ketonic and alcoholic degradation products in

phytoplankton samples from Commonwealth Bay. This involved ultrasonic extraction of lipids with chloroform-MeOH-water (1:2:0.8, v/v/v), separation of the supernatant by centrifugation at 3500G, evaporation to dryness, and division of the residue into two equal parts. The first sub-sample was acetylated in acetic anhydride-pyridine (1:2, v/v) overnight, which converted hydroperoxides to the corresponding ketones (Mihara and Tateba, 1986), and then saponified. The second sub-sample was reduced with NaBD₄ and saponified. Comparison of the amounts of alcohols present after acetylation and NaBD₄ reduction made it possible to estimate the amount of hydroperoxides and alcohols present in the samples, while deuterium labeling (via NaBD₄ reduction) allowed us to estimate the proportion of ketones in the samples.

2.3. Derivatization

For all samples containing hydroxylic components, an aliquot was dissolved in 300 µl pyridine/bis(trimethylsilyl)trifluoroacetamide (BSTFA, Supelco; 2:1, v:v) and silylated (1 h) at 50 °C. After evaporation to dryness under a stream of N₂, the derivatized residue was dissolved in a mixture of ethyl acetate and BSTFA (to avoid desilylation) and analyzed by GC–MS, GC-QTOF or GC–MS/MS.

2.4. Assignment and quantification of lipids

Native lipids were identified and quantified using GC–MS in total ion current (TIC) or selected ion monitoring (SIM) mode using a Hewlett-Packard 5890 Series II gas chromatograph, fitted with a 30 m fused silica HP₅ms column (0.25 mm i.d., 0.25 µm film) coupled to a 5970 Series Mass Selective Detector (MSD) (Belt et al., 2012). Individual lipids (and their derivatised products) were identified on the basis of their characteristic GC retention indices (e.g. RI_{HP5ms} 2082 and 2044 for IPSO₂₅ and HBI III, respectively) and

mass spectra (Belt, 2018), together with comparison of both parameters with those obtained from purified standards (Smik et al., 2016). Quantification of individual lipids was achieved first by manual integration of GC–MS peak areas, division of these by those of the respective internal standards, and normalization of the resulting ratios using instrumental response factors obtained for each lipid (Belt et al., 2014; Smik et al., 2016). These normalised ratios were then multiplied by the mass of the internal standard and finally converted to their corresponding seawater concentrations using the volume of water filtered or mass of sediment extracted. All analytical data can be found in Supplementary Table 1.

2.5. Assignment and quantification of lipid oxidation products

Lipid oxidation products were identified by comparison of retention times, accurate masses and mass spectra with those of standards and quantified (calibration with external standards) using gas chromatography–electron ionization quadrupole time of flight mass spectrometry (GC-QTOF). GC-QTOF analyses were carried out with an Agilent 7890B/7200A GC-QTOF System (Agilent Technologies, Parc Technopolis - ZA Courtaboeuf, Les Ulis, France). A cross-linked 5% phenyl-methylpolysiloxane (Macherey Nagel; Optima 5-MS Accent) column (30 m × 0.25 mm, 0.25 µm film thickness) was employed. Analyses were performed with an injector operating in pulsed splitless mode at 280 °C and the oven temperature programmed from 70 °C to 130 °C at 20 °C min⁻¹, then to 250 °C at 5 °C min⁻¹, and then to 300 °C at 3 °C min⁻¹. The carrier gas (He) was maintained at 0.69 × 10⁵ Pa until the end of the temperature program. Instrument temperatures were 300 °C for the transfer line and 230 °C for the ion source. Accurate mass spectra were obtained across the range m/z 50-700 at 4 GHz. The QTOF-MS

instrument provided a typical resolution ranging from 8009 to 12252 from m/z 68.9955 to 501.9706. Perfluorotributylamine (PFTBA) was utilized for daily MS calibration.

2.6. Assignment and quantification of HBI oxidation products

Quantification of HBI oxidation products was carried out using an Agilent 7850-A gas chromatograph connected to an Agilent 7010-QQQ mass spectrometer working in multiple reaction monitoring (MRM) mode. The following conditions were employed: 30 m x 0.25 mm (i.d.) fused silica column coated with HP-5MS (Agilent; film thickness: 0.25 μm); oven programmed from 70 to 130 $^{\circ}\text{C}$ at 20 $^{\circ}\text{C min}^{-1}$, then to 250 $^{\circ}\text{C}$ at 5 $^{\circ}\text{C min}^{-1}$ and then to 300 $^{\circ}\text{C}$ at 3 $^{\circ}\text{C min}^{-1}$; carrier gas (He), 1.0 bar; injector (splitless), 250 $^{\circ}\text{C}$; electron energy, 70 eV; source temperature, 230 $^{\circ}\text{C}$; quadrupole temperature, 150 $^{\circ}\text{C}$; scan range m/z 40-700; collision energy, ranging from 5 to 15 eV; collision flow, 1.5 ml min^{-1} (N_2); quench flow, 2.25 ml min^{-1} (He); cycle time, 0.2 s. Oxidation products were assigned by comparison of retention times and mass spectra with those of standards. Due to the presence of two highly photo-reactive tri-substituted double bonds (C-7/20 and C-9/10) in HBI III (**2**), it was not possible to quantify its primary oxidation products directly using standards, since they are not accumulated due to rapid further oxidation (Rontani et al., 2014a). We therefore quantified photoproducts of a related HBI triene **3** (possessing only one reactive tri-substituted double bond (C-9/10); see appendix) as an external standard and estimated the quantities of oxidation products from the triene **2** by applying a correction factor (Rontani et al., 2014b).

2.7. Standard compounds

The synthesis of 3-methylidene-7,11,15-trimethylhexadecan-1,2-diol (phytyldiol) (**7**) was described previously by Rontani and Aubert (2005). (8-11)-Hydroperoxyhexadec-(8-

10)-enoic acids (*Z* and *E*) (**36-41**) and (8-11)-Hydroperoxyoctadec-(8-10)-enoic (*Z* and *E*) (**30-35**) acids were produced by Fe²⁺/ascorbate-induced autoxidation (Loidl-Stahlhofen and Spiteller, 1994) of palmitoleic and oleic acids, respectively. Subsequent reduction of these different hydroperoxides in methanol with excess NaBH₄ afforded the corresponding hydroxyacids. 3,6-Dihydroxy-cholest-4-ene (**18**) (employed for sterol photooxidation estimates) was obtained from Maybridge Ltd. Treatment of sitosterol (**42**) with meta-chloroperoxy-benzoic acid in dry DCM yielded a mixture of 5 α ,6 α -and 5 β ,6 β -epoxides. Heating of these epoxides in the presence of water afforded the corresponding 24-ethylcholesta-3 β ,5 α ,6 β -triol (**43**) (Holland and Diakow, 1979). IPSO₂₅ (**1**) and HBI triene **3** were purified from cultures of *Haslea ostrearia* (Belt et al., 1996; Johns et al., 1999), while HBI triene **2** was obtained from a culture of *Pleurosigma intermedium* (Belt et al., 2000). Photosensitized oxidation products (hydroperoxides) of these HBI alkenes were produced in pyridine in the presence of haematoporphyrin as photosensitizer and then reduced with NaBH₄ to the corresponding alcohols (Rontani et al., 2014a).

2.8 Diatom taxonomy

Diatom identification and enumeration were carried out for selected water and sediment samples. Specifically, three water samples of 200 ml each were collected at CTD015 (5, 40, 563 m). Overlying bottom water (100 μ l), diatomaceous fluff (50 μ l) and sediment samples were collected from MC061. Sediment was also collected from MC045. The water samples were immediately fixed with Lugol's solution (~0.5 ml). Back at the laboratory, the preserved water samples were concentrated (CTD015) or diluted (MC061) into Utermöhl chambers to a final volume of 3 ml. After sedimentation of 48 hrs, a minimum total of 400 cells (including microphyto- and microzooplankton live at the time of preservation), were identified and counted following the Utermöhl method (Utermöhl,

1958) at a magnification of 400x under an inverted microscope (Olympus IMT-2, Japan). Microplankton were identified to species level where possible using appropriate taxonomic literature (Hasle, 1965; Tomas, 1997; Scott and Marchant, 2005, Kim et al. 2013). Final counts were converted to cells l⁻¹. Sediment samples were dried at 50 °C. Quantitative slides were made using a settling method (Scherer, 1994). Approximately 5 ml of water and hydrogen peroxide was added to several mg of each sample, and the samples were placed on a warming tray at 50 °C for 2–3 days. After complete reaction and removal of organic material, the samples were poured into water-filled 1 l beakers and allowed to settle onto coverslips. The coverslips were mounted on glass slides using Norland Optical Adhesive #61 cured under UV light. These quantitative slides were used for assessment of the diatom assemblage, by identification and counting of a minimum of 400 diatom valves along cross-slide transects, at a magnification of 1000x. Counting followed the method described by Schrader and Gersonde (1978) and Crosta and Koc (2007). Diatom concentration (diatom valves per gram) and relative abundance (percentage) of diatom species were calculated.

For the purposes of the current investigation, we determined the distribution of three common *Fragilariopsis* spp. to provide a semi-quantitative assessment of the relative contribution from sea ice-associated (*F. curta* and *F. cylindrus*) and open water (*F. kerguelensis*) diatoms. (Armand et al., 2005; Crosta et al., 2005; Crosta et al., 2008). Thus, the ratio (*F. curta* + *F. cylindrus*)/*F. kerguelensis* was determined (Table 2).

3. Results and discussion

The identification and quantification of the various lipids and their degradation products are described here according to the individual lipid classes at each sampling location. The sequence of presentation is arranged so as to first provide sufficient evidence

for the oxidation state of the lipids, in order that the variability in the ratio of IPSO₂₅ (1)/HBI III (2) can then be put into context.

3.1. Lipids and their degradation products in water samples from west of the Dalton Iceberg Tongue

3.1.1. Chlorophyll phytol side-chain

In addition to phytol (4), which mainly arises from the hydrolysis of the chlorophyll phytol side-chain during alkaline hydrolysis, significant amounts of 3,7,11,15-tetramethylhexadecanoic acid (phytanic acid) (5), 3,7,11,15-tetramethylhexadec-1-en-ol-3 (isophytol) (6) and 3-methylidene-7,11,15-trimethylhexadecan-1,2-diol (phytyldiol) (7) could also be detected in the different samples. However, phytanic acid (5) was not quantified in the present work due to its lack of specificity. Indeed, this isoprenoid acid is also formed during the aerobic and anaerobic bacterial degradation of phytol (Rontani and Volkman, 2003) and the grazing of phytoplankton (Prah et al., 1984).

In contrast, there have been very few reports of the presence of isophytol (6) in the marine environment (Fang et al., 2006), so its relatively high proportion compared to phytol (1) in some samples (Table 1) is potentially surprising. Isophytol (6) may be formed in sediments either by enzyme-catalyzed allylic rearrangement during bacterial degradation of phytol under denitrifying conditions (Rontani et al., 1999), or by clay-catalyzed dehydration of phytol (de Leeuw et al., 1974). It is interesting to note that relatively high proportions of isophytol were also recently observed after NaBH₄-reduction and alkaline hydrolysis of phytoplanktonic cells collected from Commonwealth Bay, Antarctica (Rontani and Galeron, 2016). In order to explain this observation, it was proposed that

allylation (Berkessel, 2009) of the chlorophyll phytyl side-chain by peroxy radicals could result in the formation of the precursor 3-peroxy-3,7,11,15-tetramethylhexadec-1-ene (**8**), with subsequent reduction to isophytol (**6**) (Fig. 2) (Rontani and Galeron, 2016). The absence of the initial reduction step employed here (i.e. using NaBH₄) during conventional treatment of environmental samples is likely at the origin of the very few reports of isophytol (**6**) in previous studies. In any case, the high values of the ratio isophytol/phytol observed at station 25, and to a lesser extent at station 28B (Table 1), attest to the presence of high concentrations of peroxides, and thus of a strong photo- or autoxidation state of POM.

The formation of phytyldiol (**7**) results from initial Type II photosensitized oxidation (i.e. involving singlet oxygen (¹O₂)) of the chlorophyll phytyl side-chain and subsequent hydrolysis of the photoproducts thus formed (Rontani et al., 1994). On the basis of its high specificity and widespread occurrence in the environment (Cuny and Rontani, 1999), this diol can be used as a specific tracer of chlorophyll photodegradation. Further, Cuny et al. (2002) proposed that the amount of chlorophyll photodegradation in the marine environment could be estimated from the so-called Chlorophyll Phytyl side-chain Photodegradation Index (CPPI) derived from the molar ratio phytyldiol/phytol. Using this approach, the highest photooxidation state of POM was confirmed as being at station 25 and the lowest at station 32 (<1%, not included in the figure) (Fig. 3).

3.1.2. Sterols

The major sterols in the filtered water sample were 24-norcholest-5,22*E*-dien-3β-ol (22-dehydrocholesterol) (**10**), cholest-5-en-3β-ol (cholesterol) (**11**), 24-methylcholesta-5,22*E*-dien-3β-ol (*epi*-brassicasterol) (**12**), 24-methylcholesta-5,24(28)-dien-3β-ol (24-methylenecholesterol) (**13**) and 24-ethylcholest-7-en-3β-ol (22-dihydrocondrillasterol) (**14**)

(Supplementary Table 1). 22-Dehydrocholesterol (**10**) has been found in diatoms and notably in *Thalassiosira aff. antarctica* (Rampen et al., 2007). Although cholesterol (**11**) may be derived from diatoms or Prymnesiophycean algae (Volkman, 1986), its dominance generally suggests an important contribution of zooplanktonic faecal material to the samples. Indeed, it is well known that zooplankton convert much of the sterols produced by algae into cholesterol (**11**) (Volkman et al., 1980; Prahl et al., 1984). *Epi*-brassicasterol (**12**) and 24-methylenecholesterol (**13**) are major constituents of several diatom species (Lee et al., 1980) including sea ice diatoms (Belt et al., 2018). However, it may be noted that *epi*-brassicasterol (**12**) is also present in some dinoflagellates and in many haptophytes (Volkman, 1986, 2003). The unusual sterol 22-dihydrochondrillasterol (**14**) was detected previously in some Chlorophyceae (Martin-Creuzburg et al., 2011; Martin-Creuzburg and Merkel, 2016). The sterol profiles observed in these samples (Supplementary Table 1) are thus typical of mixed assemblages of diatoms, Prymnesiophytes and Chlorophytes.

Type II photosensitized oxidation of Δ^5 -sterols produces mainly unstable Δ^6 -5 α -hydroperoxides with low amounts of Δ^4 -6 α/β -hydroperoxides (Smith, 1981). Here, we selected Δ^4 -6 α/β -hydroperoxides as tracers of photooxidation of Δ^5 -sterols due to their high specificity and relative stability (Rontani et al., 2009; Christodoulou et al., 2009). These compounds were quantified after NaBH₄ reduction to the corresponding diols and photooxidation percentage was obtained from the equation: photooxidation % = (Δ^4 -sterol-6 α/β -diols % \times (1+0.3)/0.3) (Christodoulou et al., 2009). The values obtained for *epi*-brassicasterol (**12**) and 24-methylenecholesterol (**13**) (the two main algal sterols present in the samples analyzed) are shown in Fig. 3. Photooxidation of these two sterols exhibits the same general trend as that seen for chlorophyll, with the highest photooxidation state observed at station 25 (Fig. 3). Interestingly, as observed previously in the Arctic (Rontani et al., 2012; 2014a), photodegradation processes appeared to have acted more intensively

on 24-methylenecholesterol (**13**) (mainly arising from diatoms) than on *epi*-brassicasterol (**12**) (arising from diatoms and/or Prymnesiophytes). These differences confirm the higher efficiency of Type II photosensitized oxidation processes in diatoms compared to Prymnesiophytes.

Stanols constitute useful indicators of bacterial degradation of Δ^5 -sterols (Gagosian et al., 1982; de Leeuw and Baas, 1986; Wakeham, 1989). We thus quantified the ratio 24-methyl-5 α -cholest-22*E*-en-3 β -ol (*epi*-brassicastanol) (**15**)/*epi*-brassicasterol (**12**) to indicate the extent of bacterial degradation of algal material. (Note: the ratio 24-methyl-5 α -cholest-24(28)-en-3 β -ol (**16**)/24-methylenecholesterol (**13**) could not be quantified due to co-elution of the stanol **16** with the isobaric campesterol (**17**)). The values of the ratio *epi*-brassicastanol (**15**)/*epi*-brassicasterol (**12**) (Table 1) show only a weak increase with depth suggesting that bacterial degradation processes acted only weakly on algal material.

3.1.3. Fatty acids

The fatty acid content of the SPM samples is characterized by a very low content of polyunsaturated fatty acids (PUFAs) and notably of C_{18:4} (**19**), C_{20:5} (**20**) and C_{22:6} (**21**) acids, which are typical for marine plankton (Kattner et al., 1983). Instead, the dominant fatty acids are the saturated and monounsaturated fatty acids (MUFAs) (i.e. C_{14:0} (**22**), C_{16:1 ω 7} (palmitoleic acid) (**23**), C_{16:0} (palmitic acid) (**24**), C_{18:1 ω 9} (oleic acid) (**25**), C_{18:1 ω 7} (vaccenic acid) (**26**) and C_{18:0} (**27**)) (Supplementary Table 1). The reactivity of unsaturated fatty acids with respect to auto- and photooxidative processes increases, logically, with the number of double bonds (Frankel, 1998; Rontani et al., 1998). The very low amounts of PUFAs is therefore suggestive of intense photo- or autooxidation of the samples. In order to confirm this, the oxidation products of MUFAs (oleic and palmitoleic acids) (**25** and **23**) were quantified since they are sufficiently stable in the marine environment to act as

markers of these abiotic degradative processes (Marchand and Rontani, 2001, 2003). Photo- and autoxidation of monounsaturated fatty acids affords mixtures of isomeric allylic hydroperoxyacids (Frankel, 1998). Based on the specific formation of *cis* isomers by autoxidation (Porter et al., 1995), the relative importance of photooxidation and autoxidation can easily be distinguished by quantifying the respective hydroxyacids that result from NaBH₄-reduction of these compounds (Marchand and Rontani, 2001). The results obtained (Fig. 4) show a clear difference in reactivity between palmitoleic (**23**) and oleic (**25**) acids. Indeed, photo- and autoxidation states appeared to be considerably higher in the case of palmitoleic acid (**23**) (the main MUFA of diatoms, Fahl and Kattner, 1993; Leu et al., 2010) compared to oleic acid (**25**) (dominant in Prymnesiophytes, Rossi et al., 2006). These outcomes are consistent with previous observations of more efficient photo- and autoxidation processes in diatoms than in Prymnesiophytes (Rontani et al., 2012; 2014b). Such differences in reactivity were attributed previously to the involvement of intra-cellular compartmentalization effects, which may significantly modify the reactivity of lipids towards autoxidative and photooxidative processes according to their location in phytoplanktonic cells (Rontani, 2012).

The palmitoleic (**23**)/palmitic acid (**24**) ratio is often employed to follow diatom blooms (Pedersen et al., 1999; Reuss and Poulsen, 2002). Due to the strong oxidation of palmitoleic acid (**23**) observed in some of our samples (Fig. 4), we employed the ratio (Σ palmitoleic acid (**23**) and its oxidation products)/palmitic acid (**24**) to estimate the relative proportion of diatom in the mixed phytoplankton assemblages. Using this approach, we observed a relatively high proportion of (strongly oxidized) diatoms in the surface water sample of station 25 and an increase in their proportion with water depth at station 28B (Table 1).

3.1.4. Cutin components

Relatively high amounts of 9,16-dihydroxyhexadecanoic (**29**) and 10,16-dihydroxyhexadecanoic (**28**) acids were observed in some samples (Table 1). These compounds are well-known depolymerisation products of cutins (insoluble polyester polymers) present in the outer layer of the epidermal cells of primary plant tissues, such as leaves) (Deas and Holloway, 1977; Kolattukudy, 1977, 1980). The presence of such compounds is very surprising since the Antarctic biome is an unfavorable environment for higher plant growth. Only two native phanerogams, *Deschampsia antarctica* Desv. and *Colobanthus quitensis* (Kunth) Bartl., occur in Antarctica to almost 69°S (Smith 1994). The high concentrations of dihydroxyacids **28** and **29** detected in some sub-surface water samples (Table 1) is therefore attributed to the accumulation of low density debris of such plants.

3.1.5. HBI alkenes

The two HBI lipids, IPSO₂₅ (**1**) and HBI III (**2**), reported previously by Smik et al. (2016) in the surface water samples described here, were also present in each of the sub-surface and deep water samples investigated for the first time within the current study. Although there was some variability in the absolute and relative concentrations of these HBIs between the surface and sub-surface samples, The IPSO₂₅ (**1**)/HBI III (**2**) ratio was mainly slightly higher in the majority of the sub-surface samples compared to the surface water counterparts, with CTD-004 and -014 the only exceptions. More striking changes to this ratio were observed with the corresponding deep water samples, however, with mean (i.e. across all samples) relative enhancements in IPSO₂₅ (**1**)/HBI III (**2**) of ca. 8 and 6 when compared with the surface and sub-surface samples, respectively (Table 1).

The systematic increase of the ratio **1/2** with depth (Table 1) may potentially be attributed to: (i) a relatively higher contribution of ice algae (and thus IPSO₂₅ (**1**)) to the deeper samples resulting from their stronger aggregation and therefore higher sinking rate, or (ii) a stronger abiotic degradation of HBI III (**2**) during settling through the water column. One characteristic of sea ice algae is their ability to produce high amounts of extracellular polymeric substances (EPS); the production of which facilitates the attachment of algae to their substrate (sea ice) but also allows the formation of aggregates of algal cells (Riebesell, 1991; Alldredge et al., 1993; Passow, 2002), thus shortening their residence time within the euphotic zone. In the case of station 28B, the simultaneous increase of the ratios **1/2** and (Σ palmitoleic acid (**23**) and its oxidation products)/palmitic acid (**24**) with depth (Table 2) suggests a dominance of aggregated ice diatom material in the deepest SPM sample.

Photo- and autoxidation of IPSO₂₅ (**1**) were previously studied in vitro (Rontani et al., 2011; 2014a). Based on its very low degradation rates (resulting from the poor reactivity of its two terminal double bonds (i.e. at C6-17 and C23-24) towards ¹O₂ and free radicals), it is feasible that this diene (**1**) could be largely unaffected by abiotic oxidation within the water column of the oceans, at least in comparison with some more unsaturated lipids, or those containing more reactive double bonds. Indeed, HBI triene **2** possesses two tri-substituted double bonds (i.e. at C7–20 and C9–10), both of which are more reactive towards ¹O₂ (Frimer, 1983) than the two double bonds in IPSO₂₅. In addition, the relative positions of these two double bonds in HBI III (**2**) creates a bis-allylic methylene group (at C-8) that can lose a hydrogen atom even more readily (Yin et al., 2011). HBI triene **2** is thus very sensitive towards photo- and autoxidation processes and exhibits degradation rates close to those of PUFAs (Rontani et al., 2014a). On the basis of the very intense abiotic alteration of these fatty acids in the samples investigated here (see section 3.1.3), a

similar oxidation of HBI triene (**2**) was thus expected. However, we were not able to detect the previously identified primary oxidation products of **2** (Rontani et al., 2014a), probably due to their further oxidation to polar and oligomeric compounds, which are not generally detectable using the GC–MS methods employed here. This conclusion is consistent with the strong photo- and autooxidation states of palmitoleic acid (**23**) observed in these samples (Fig. 4) and the differences of reactivity observed previously between HBI III (**2**) and this acid in diatom cells ($k_{\text{photo HBI III}}/k_{\text{photo palmitoleic acid}} \approx 4$ and $k_{\text{auto HBI III}}/k_{\text{auto palmitoleic acid}} > 10$) (Rontani et al., 2011; 2014a).

In order to provide further evidence for the influence of autooxidative processes upon the ratio **1/2**, we measured it, together with the autooxidation state of sitosterol (**42**) (estimated on the basis of $3\beta,5\alpha,6\beta$ -trihydroxysitosterol (**43**) as previously proposed by Christodoulou et al. (2009)) and palmitoleic acid (**23**) in the water column samples from station 32 (T32/CTD015) and in two near-surface sediment samples from nearby locations (MC45 and MC61; Fig. 1), with one of these (MC61) located directly at the station where the CTD015 samples were taken. The ratio **1/2** was also measured in the surface waters recovered from the top of the MC61 sediment core and in the suspension of diatomaceous ‘fluff’ taken at the water-sediment interface, thereby providing a near-continuous depth sequence from surface waters to underlying sediments. Although sitosterol (**42**) is commonly associated with higher plants ((Lütjohann, 2004), it is also present in phytoplankton, and notably in diatoms (Volkman, 1986; 2003). Due to the absence of lipid signatures of terrestrial material in the water samples collected at station 32 and in the sediments from nearby locations, the presence of sitosterol (**42**) in these samples was thus attributed to an algal origin. The results obtained (Table 2) show a clear increase in both the ratio **1/2** and the autooxidation state of algal material with water depth and then into the surface sediments (Table 2). The failure to detect oxidation products of sitosterol in the

water column samples is attributed to the relatively poor chromatographic properties of the only partially silylated (at positions 3 and 6) triol **43**, which hinders its detection at low concentrations.

Although we do not currently have detailed taxonomic data from all sampling stations/types, we do have data from the station for which we have lipid profiles from both the water column and underlying Megacore (viz. CTD015 & MC61). The most striking feature is the consistent decrease in the ratio (*F. curta* + *F. cylindrus*)/*F. kerguelensis* through the water column, the water-sediment interface and then into the sub-surface sediment (Table 2), suggesting a progressive decrease in the relative contribution of sea ice-associated and open-water diatoms. However, this conclusion is contrary to what might be inferred from the (increasing) IPSO₂₅ (**1**) /HBI III (**2**) ratio, suggesting that changes in the latter, at some locations, are determined more by the enhanced degradation of HBI III (relative to IPSO₂₅) as shown from the lipid data described above; the caveat being that the aforementioned *Fragilariopsis* spp. are not known HBI-producers. We also assume that the water column data derived from samples taken in a single sampling season are also representative of multi-annual accumulation that the sediment samples likely reflect. Unfortunately, the known sources of IPSO₂₅ and HBI III were of too low abundance for more direct comparisons between lipid and taxonomic distributions to be made for these samples. Interestingly, a positive relationship between IPSO₂₅ (**1**)/HBI triene (**2**) and the ratio *F. curta*/*F. kerguelensis* (i.e., a slight modification to our diatom ratio) was reported in a previous downcore sediment study from the region (Massé et al., 2011), suggesting that the modifications to the former described herein for the water column and water-sediment interface may not necessarily have an adverse impact on its use as a proxy measure of sea ice change in palaeo records, especially for qualitative purposes. Further studies comparing these two approaches will, however, be required, before the generality

of this observation can be confirmed, and the most reliable use of IPSO₂₅/HBI III as a proxy measure of sea ice change can be deciphered.

3.2. Phytoplanktonic material from Commonwealth Bay (East Antarctica)

To demonstrate the efficiency of photo- and autoxidation processes on HBI III (**2**) in this region, more generally, we also analysed phytoplanktonic cells collected from surface waters of Commonwealth Bay (also East Antarctica; see Fig. 1). In this weakly oxidized material (oxidation percentage of palmitoleic acid (**23**) < 5%), MRM analyses allowed us to detect the HBI alcohols **44–48** (Figs. 5B and 6B, Table 3). The assignment of these compounds was confirmed by comparison with the MRM chromatograms of standards obtained by photo- and autoxidation of HBI III (**2**) (Figs. 5A and 6A) (Rontani et al., 2014b). Alcohol **48** is produced specifically by photooxidation of HBI III (**2**), while alcohols **44–47** result from both its photo- and autoxidation (Rontani et al., 2014a). On the basis of the detection of these oxidation products in a weakly oxidized phytoplanktonic sample from Commonwealth Bay, the strong increase of the ratio IPSO₂₅ (**1**)/HBI III (**2**) observed in the deeper SPM samples from stations 25, 27, 32 and 34 and in near-surface sediments from the polynya region west of the Dalton Iceberg Tongue (Tables 1 and 2) may be thus attributed to an intense photo- and/or autoxidation of HBI III (**2**) within the water column, with further autoxidation of (**2**), relative to (**1**), at the water-sediment interface and in the oxic layer of the underlying sediment.

During the NaBH₄-reduction step employed to avoid thermal degradation of hydroperoxides during the subsequent saponification reaction, the sum of hydroperoxides and their degradation products (alcohols and ketones) was obtained via quantification of their respective alcohols. Two different treatments were employed (acetylation and saponification vs NaBD₄-reduction and saponification) (see Section 2.2) in order to

specifically quantify hydroperoxides and their main degradation products (i.e. alcohols and ketones). The results obtained (summarized in Table 4) show that a substantial proportion (ca. 55–81%) of HBI III (**2**) oxidation products were still present as hydroperoxides.

Interestingly, the decrease in unlabeled phytol (**4**) concentration (5–20%) observed when the treatment of phytoplanktonic cells involved acetylation and saponification instead of NaBD₄-reduction and saponification, provides further evidence for the formation pathway of isophytol (**6**) proposed previously (Rontani and Galeron, 2016) (Fig. 2). Indeed, this decrease likely results from the presence of 1-peroxy-3,7,11,15-tetramethylhexadec-3-ene (**9**), which is formed by allylic rearrangement of its isomer **8** (Fig. 2).

4. Conclusions

Selected lipids and their oxidation products were quantified in SPM samples collected at different water depths in the polynya region west of the Dalton Iceberg Tongue (East Antarctica). The sterol profiles were typical of mixed assemblages of diatoms, prymnesiophytes and chlorophytes. Surprisingly, some samples contained depolymerisation products of cutins, the presence of which was attributed to the accumulation of low-density debris of the two phanerogams present in Antarctica.

We identified an intense photo- and autoxidation of unsaturated diatom components (e.g. palmitoleic acid (**23**), 24-methylenecholesterol (**13**), chlorophyll phytyl side-chain (**4**)), but not of the HBI triene **2**, despite its known reactivity towards such processes, likely due to its susceptibility towards further oxidation. However, oxidation products of HBI triene (**2**) could be detected in weakly oxidized SPM samples collected from Commonwealth Bay (East Antarctica), clearly demonstrating the oxidation of this lipid in this region.

The systematic increase of the ratio IPSO₂₅ (1)/HBI triene (2) observed with depth in the water column and in some underlying sediments thus appears to result, in part, from an intense and preferential abiotic degradation of the HBI triene (2) due to a combination of photo- and autoxidation processes. At one sampling site, the increase in the IPSO₂₅ (1)/HBI triene (2) ratio with depth was opposite to that of the ratio of selected sea ice-associated versus open-water diatoms, suggesting that the differential biomarker degradation was a dominant factor. However, for another sampling site, the increase in the IPSO₂₅ (1)/HBI triene (2) ratio appeared to be more influenced by the accumulation of ice algal material, although we do not yet have the complementary taxonomic data to confirm this.

Distinguishing between these two factors will require more detailed and combined lipid and taxonomic analysis in the future. In the meantime, it is evident from the results presented here, that the differential degradation of IPSO₂₅ (2) and HBI triene (3) in the water column and in near-surface sediments (at least) can impact on the ratio between these two HBIs between their source and sedimentary environments. The latter should be taken into account when using this parameter for palaeo sea ice reconstruction purposes in the Antarctic. The extent to which the IPSO₂₅ (1)/HBI triene (2) ratio reflects established proxy measures of past sea ice change (e.g., the ratio of certain *Fragilariopsis* spp. as described herein) will require more studies of both parameters in further downcore records from the Antarctic.

Acknowledgements

The FEDER OCEANOMED (N° 1166-39417) is acknowledged for the funding of the apparatus employed. Thanks are due to the scientific party and crew of cruise NBP1402;

the project (P.I. A. Leventer) was funded by NSF ANT-1143836. We also thank G. Massé for the donation of the phytoplankton samples collected in the Commonwealth Bay during the IPEV-COCA2012 cruise funded by IPEV (1010-ICELIPIDS program) and ANR (CLIMICE program).

References

- Aldredge, A.L., Passow, U., Logan, B.E., 1993. The abundance and significance of a class of large, transparent organic particles in the ocean. *Deep-Sea Research Part I-Oceanographic Research Papers* 40, 1131-1140.
- Armand, L., Crosta, X., Romero, O., Pichon, J.J., 2005. The biogeography of major diatom taxa in Southern Ocean sediments.1. Sea ice related species. *Palaeogeography, Palaeoclimatology, Palaeoecology* 223, 93–126.
- Armand, L.K., Ferry, A., Leventer, A., 2017. Advances in palaeo sea ice estimation. In: Thomas, D.N. (Ed.), *Sea Ice*. John Wiley & Sons Ltd, Chichester, pp. 600–629.
- Barbara, L., Crosta, X., Massé, G., Ther, O., 2010. Deglacial environments in eastern Prydz Bay, East Antarctica. *Quaternary Science Reviews* 29, 2731–2740.
- Barbara, L., Crosta, X., Schmidt, S., Massé, G., 2013. Diatoms and biomarkers evidence for major changes in sea ice conditions prior the instrumental period in Antarctic Peninsula. *Quaternary Science Reviews* 79, 99–110.
- Barbara, L., Crosta, X., Leventer, A., Schmidt, S., Etourneau, J., Domack, E., Massé, G., 2016. Environmental responses of the Northeast Antarctic Peninsula to the Holocene climate variability, *Paleoceanography*, 31, 131–147.

- Belt, S.T., Cooke, D.A., Robert, J.-M., Rowland, S.J., 1996. Structural characterisation of widespread polyunsaturated isoprenoid biomarkers: A C₂₅ triene, tetraene and pentaene from the diatom *Haslea ostrearia* Simonsen. *Tetrahedron Letters* 37, 4755–4758.
- Belt, S.T., Allard, W.G., Massé, G., Robert, J.-M., Rowland, S.J., 2000. Highly branched isoprenoids (HBIs): identification of the most common and abundant sedimentary isomers. *Geochimica et Cosmochimica Acta* 64, 3839–3851.
- Belt, S.T., Massé, G., Rowland, S.J., Poulin, M., Michel, C., LeBlanc, B., 2007. A novel chemical fossil of palaeo sea ice: IP₂₅. *Organic Geochemistry* 38, 16–27.
- Belt, S.T., Müller, J., 2013. The Arctic sea ice biomarker IP₂₅: a review of current understanding, recommendations for future research and applications in palaeo sea ice reconstructions. *Quaternary Science Reviews* 79, 9–25.
- Belt, S.T., Brown, T.A., Ampel, L., Cabedo-Sanz, P., Fahl, K., Kocis, J.J., Masse, G., Navarro-Rodriguez, A., Ruan, J., Xu, Y., 2014. An inter-laboratory investigation of the Arctic sea ice biomarker proxy IP₂₅ in marine sediments: key outcomes and recommendations. *Climate of the Past* 10, 155–166.
- Belt, S.T., Cabedo-Sanz, P., Smik, L., Navarro-Rodriguez, A., Berben, S.M.P., Knies, J., Husum, K., 2015. Identification of paleo Arctic winter sea ice limits and the marginal ice zone: Optimised biomarker-based reconstructions of late Quaternary Arctic sea ice. *Earth and Planetary Science Letters* 431, 127–139.
- Belt, S.T., Smik, L., Brown, T.A., Kim, J.H., Rowland, S.J., Allen, C.S., Gal, J.K., Shin, K.H., Lee, J.I., Taylor, K.W.R., 2016. Source identification and distribution reveals the potential of the geochemical Antarctic sea ice proxy IPSO₂₅. *Nature Communications* 7, 12655.

- Belt, S.T., Brown, T.A., Smik, L., Assmy, P., Mundy, C.J., 2018. Sterol identification in floating Arctic sea ice algal aggregates and the Antarctic sea ice diatom *Berkeleya adeliensis*. *Organic Geochemistry* 118, 1–3.
- Belt, S.T., 2018. Source-specific biomarkers as proxies for Arctic and Antarctic sea ice. *Organic Geochemistry* 125, 273-295.
- Berkessel, A., 2014. *Science of Synthesis: Houben-Weyl Methods of Molecular Transformations*, Vol. 38: Peroxides, Georg Thieme Verlag, p. 75.
- Brown, T.A., Belt, S.T., Tatarek, A., Mundy, C.J., 2014c. Source identification of the Arctic sea ice proxy IP₂₅. *Nature Communications* 5, 4197.
- Campagne, P., Costa, X., Houssais, M.N., Swingedouw, D., Schmidt, S., Martin, A., Devred, E., Capo, S., Marieu, V., Closset, I., Massé, G., 2015. Glacial ice and atmospheric forcing on the Mertz Glacier Polynya over the past 250 years. *Nature Communications* 6, 6642.
- Campagne, P., Crosta, X., Schmidt, S., Houssais, M.N., Ther, O., Massé, G., 2016. Sedimentary response to sea ice and atmospheric variability over the instrumental period off Adélie Land, East Antarctica. *Biogeosciences* 13, 4205–4218.
- Christodoulou S., Marty J.-C., Miquel J.-C., Volkman J.K., Rontani J.-F., 2009. Use of lipids and their degradation products as biomarkers for carbon cycling in the northwestern Mediterranean Sea. *Marine Chemistry* 113, 25-40.
- Collins, L.G., Allen, C.S., Pike, J., Hodgson, D.A., Weckström, K., Massé, G., 2013. Evaluating highly branched isoprenoid (HBI) biomarkers as a novel Antarctic sea-ice proxy in deep ocean glacial age sediments. *Quaternary Science Reviews* 79, 87–98.
- Crosta, X., Koc, N., 2007. Diatoms: From micropaleontology to isotope geochemistry, in: *Methods in Late Cenozoic Paleoceanography*, Hilaire-Marcel, C. and de Vernal, A. (Eds.), Elsevier, Amsterdam, the Netherlands, pp. 327–369.

- 670 Crosta, X., Romero, O., Armand, L., Pichon, J.J., 2005. The biogeography of major diatom
671 taxa in Southern Ocean sediments. 2. Open Ocean related species. *Palaeogeography,*
672 *Palaeoclimatology, Palaeoecology* 223, 66–92.
- 673 Crosta, X., Denis, D., Ther, O., 2008. Sea ice seasonality during the Holocene, Adelie
674 Land, East Antarctica. *Marine Micropaleontology* 66, 222–232.
- 675 Cuny, P., Rontani, J.-F., 1999. On the widespread occurrence of 3-methylidene-7,11,15-
676 trimethylhexadecan-1,2-diol in the marine environment: a specific isoprenoid marker
677 of chlorophyll photodegradation. *Marine Chemistry* 65, 155-165.
- 678 Cuny, P., Marty, J.-C., Chiaverini, J., Vescovoli, I., Raphel, D., Rontani, J.-F., 2002. One-
679 year seasonal survey of the chlorophyll photodegradation process in the Northwestern
680 Mediterranean Sea. *Deep-Sea Research II* 49, 1987-2005.
- 681 Deas, A.H.B., Holloway, P.J., 1977. The intermolecular structure of some plant cutins. In:
682 Tevini, M., Lichtenthaler, H. (Eds.), *Lipids and Lipid Polymers in Higher Plants.*
683 Springer, Berlin, pp. 293-299.
- 684 Denis, D., Crosta, X., Barbara, L., Massé, G., Renssen, H., Ther, O., Giraudeau, J., 2010.
685 Sea ice and wind variability during the Holocene in East Antarctica: insight on
686 middle-high latitude coupling. *Quaternary Science Reviews* 29, 3709–3719.
- 687 de Leeuw, J.W., Correia, V.A., Schenck, P.A., 1974. On the decomposition of phytol under
688 simulated geological conditions and in the top-layer of natural sediments. In: Tissot,
689 B., Biennier, F. (Eds.), *Advances in Organic Geochemistry 1973.* Editions Technip,
690 Paris, pp. 993–1004.
- 691 de Leeuw, J.W., Baas, M., 1986. Early-stage diagenesis of steroids. In: Johns, R.B. (Ed.),
692 *Biological Markers in the Sedimentary Record.* Elsevier, Amsterdam, pp. 101-123.

- de Vernal, A., Gersonde, R., Goosse, H., Seidenkrantz, M.-S., Wolff, E.W., 2013. Sea ice in the paleoclimate system: the challenge of reconstructing sea ice from proxies – an introduction. *Quaternary Science Reviews* 79, 1–8.
- Dickson, R., Rudels, B., Dye, S., Karcher, M., Meincke, J., Yashayaev, I., 2007. Current estimates of freshwater flux through Arctic and subarctic seas. *Progress in Oceanography* 73, 210–230.
- Etourneau, J., Collins, L.G., Willmott, V., Kim, J.H., Barbara, L., Leventer, A., Schouten, S., Sinninghe Damsté, J.S., Bianchini, A., Klein, V., Crosta, X., Massé, G., 2013. Holocene climate variations in the western Antarctic Peninsula: evidence for sea ice extent predominantly controlled by changes in insolation and ENSO variability. *Climate of the Past* 9, 1431–1446.
- Fahl, K., Kattner, G., 1993. Lipid content and fatty acid composition of algal communities in sea-ice and water from Weddell Sea (Antarctica). *Polar Biology* 13, 405-409.
- Fang, J., Chan, O., Joeckel, R.M., Huang, Y., Wang, Y., Bazylinski, D.A., Moorman, T.B., Ang Clement, B.J., 2006. Biomarker analysis of microbial diversity in sediments of a saline groundwater seep of Salt Basin, Nebraska. *Organic Geochemistry* 37, 912-931.
- Fetterer F., Knowles K., Meier W.N., Savoie M., 2016. Sea Ice Index. ver.2 NSIDC: National Snow and Ice Data Center. Boulder, Colorado (<https://doi.org/10.7265/N5736NV7>) [Digital Media, updated daily].
- IPCC, 2013: Summary for Policymakers. In: *Climate Change 2013: The Physical Science Basis. Contribution of Working Group I to the Fifth Assessment Report of the Intergovernmental Panel on Climate Change* [Stocker, T.F., D. Qin, G.-K. Plattner, M. Tignor, S.K. Allen, J. Boschung, A. Nauels, Y. Xia, V. Bex and P.M. Midgley (eds.)]. Cambridge University Press, Cambridge, United Kingdom and New York, NY, USA.
- Frankel, E.N., 1998. *Lipid Oxidation*. The Oily Press, Dundee.

- Frimer, A.A., 1979. The reaction of singlet oxygen with olefins: the question of mechanism. *Chemical Review* 79, 359-387.
- Gagosian, R.B., Smith, S.O., Nigrelli, G.E., 1982. Vertical transport of steroid alcohols and ketones measured in a sediment trap experiment in the equatorial Atlantic Ocean. *Geochimica et Cosmochimica Acta* 46, 1163-1172.
- Hasle, G.R., 1965. *Nitzschia* and *Fragilariopsis* species studied in the light and electron microscopes III. The genus *Fragilariopsis*. *Skr. Norske Vidensk-Akad. I. Mat.-Nat. Kl. Ny Serie* 21, 1–49.
- Holland, H.L., Diakow, P.R.P., 1979. Microbial hydroxylation of steroids. 5. Metabolism of androst-5-en-3,17-dione and related compounds by *Rhizopus arrhizus* ATCC 11145. *Canadian Journal of Chemistry* 57, 436-440.
- Johns, L., Wraige, E.J., Belt, S.T., Lewis, C.A., Massé, G., Robert, J.M., Rowland, S.J., 1999. Identification of a C₂₅ highly branched isoprenoid (HBI) diene in Antarctic sediments, Antarctic sea-ice diatoms and cultured diatoms. *Organic Geochemistry* 30, 1471–1475.
- Kattner, G., Cercken, G., Eberlein, K., 1983. Development of lipid during a spring bloom in the northern North Sea. I. Particulate fatty acids. *Marine Chemistry* 14, 149-162.
- Kim, S.Y., Choi, J.K., Dolan, J.R., Shin, H.C., Lee, S., Yang, E.J., 2013. Morphological and ribosomal DNA-based characterization of six Antarctic ciliate morphospecies from the Amundsen Sea with phylogenetic analyses. *Journal of Eukaryotic Microbiology* 60, 497-513.
- Kolattukudy, P.E., 1977. Lipid polymers and associated phenols, their chemistry, biosynthesis, and role in pathogenesis, *Recent Advances in Phytochemistry* 77, 185-246.

- Kolattukudy, P.E., 1980. Cutin, suberin and waxes. In: Stumpf, P.K., Conn, E.E. (Eds.),
The Biochemistry of Plants, vol. 4. Academic Press, Davis, pp. 571–645.
- Lee, C., Gagosian, R.B., Farrington, J.W., 1980. Geochemistry of sterols in sediments from
Black Sea and the southwest African shelf and slope, Organic Geochemistry 2, 103-
113.
- Leventer, A., 2013. The fate of Antarctic “sea ice diatoms” and their use as
paleoenvironmental indicators. In: Lizotte, M.P., Arrigo, K.R. (Eds.), Antarctic Sea
Ice: Biological processes, Interactions and Variability. American Geophysical Union,
pp. 121–137.
- Leventer, A., Armand, L., Harwood, D.M., Jordan, R., Ligowski, R., 2008. New
approaches and progress in the use of polar marine diatoms in reconstructing sea ice
distribution. Papers in the Earth and Atmospheric Sciences. Paper 287.
- Leventer, A., 1998. The fate of sea ice diatoms and their use as paleoenvironmental
indicators. In: Lizotte, M.P. and Arrigo, K.R. (Eds.), Antarctic Sea Ice: Biological
Processes, AGU Research Series 73, Washington, D.C., pp. 121–137.
- Leu, E., Wiktor, J., Soreide, J.E., Berge, J., Falk-Petersen, S., 2010. Increased irradiance
reduces food quality of sea ice algae. Marine Ecology Progress Series 411, 49-60.
- Loidl-Stahlhofen, A., Spiteller, G., 1994. α -Hydroxyaldehydes, products of lipid
peroxidation. Biochimica et Biophysica Acta 1211, 156-160.
- Lütjohann, D., 2004. Sterol autoxidation: from phytosterols to oxyphytosterols. British
Journal of Nutrition 91, 3-4.
- Marchand, D., Rontani, J.-F., 2001. Characterisation of photooxidation and autoxidation
products of phytoplanktonic monounsaturated fatty acids in marine particulate matter
and recent sediments. Organic Geochemistry 32, 287-304.

- Marchand, D., Rontani, J.-F., 2003. Visible light-induced oxidation of lipid components of purple sulfur bacteria: a significant process in microbial mats. *Organic Geochemistry* 34, 61-79.
- Martin-Creuzburg, D., Beck, B., Freese, H.M., 2011. Food quality of heterotrophic bacteria for *Daphnia magna*: evidence for a limitation by sterols. *FEMS Microbiology* 76, 592-601.
- Martin-Creuzburg, D., Merkel, P., 2016. Sterols of freshwater microalgae: potential implications for zooplankton nutrition. *Journal of Plankton Research* 38, 865-877.
- Mihara, S., Tateba, H., 1986. Photosensitized oxygenation reactions of phytol and its derivatives. *The Journal of Organic Chemistry* 51, 1142-1144.
- Passow, U., 2002. Transparent exopolymer particles (TEP) in aquatic environments. *Progress in Oceanography* 55, 287-333.
- Pedersen, L., Jensen, H.M., Burmeister, A.D., Hansen, B.W., 1999. The significance of food web structure for the condition and tracer lipid content of juvenile snail fish (Pisces: Liparis spp.) along 65–728N off West Greenland. *Journal of Plankton Research* 21, 1593-1611.
- Perette, M., Yool, A., Quartly, G.D., Popova, E.E., 2011. Near-ubiquity of ice-edge blooms in the Arctic. *Biogeosciences* 8, 515–524.
- Porter, N.A., Caldwell, S.E., Mills, K.A., 1995. Mechanisms of free radical oxidation of unsaturated lipids. *Lipids* 30, 277-290.
- Prahl, F.G., Eglinton, G., Corner, E.D.S., O’Hara, S.C.M., Forsberg, T.E.V., 1984. Changes in plant lipids during passage through the gut of *Calanus*. *Journal of the Marine Biological Association of the United Kingdom* 64, 317-334.

- Reuss, N., Poulsen, L.K., 2002. Evaluation of fatty acids as biomarkers for a natural plankton community. A field study of a spring bloom and a post-bloom period off West Greenland. *Marine Biology* 141, 423-434.
- Riebesell U., Schloss I., Smetacek V., 1991. Aggregation of algae released from melting sea ice-implications for seeding and sedimentation. *Polar Biology* 11,239-248.
- Rampen, S.W., Abbas, B.A., Schouten, S., Sinninghe Damsté, J.S., 2010. A comprehensive study of sterols in marine diatoms (Bacillariophyta): implications for their use as tracers for diatom productivity. *Limnology and Oceanography* 55, 91–105.
- Rontani, J.-F., Grossi, V., Faure, F., Aubert, C., 1994. ‘‘Bound’’ 3-methylidene-7,11,15-trimethylhexadecan-1,2-diol: a new isoprenoid marker for the photodegradation of chlorophyll-a in seawater. *Organic Geochemistry* 21, 135-142.
- Rontani, J.-F., Cuny, P., Grossi, V., 1998. Identification of a pool of lipid photoproducts in senescent phytoplanktonic cells. *Organic Geochemistry* 29, 1215-1225.
- Rontani, J.-F., Bonin, P., Volkman, J.K., 1999. Biodegradation of free phytol by bacterial communities isolated from marine sediments under aerobic and denitrifying conditions. *Applied and Environmental Microbiology* 65, 5484–5492.
- Rontani, J.-F., Volkman, J.K., 2003. Phytol degradation products as biogeochemical tracers in aquatic environments. *Organic Geochemistry* 34, 1-35.
- Rontani, J.-F., Aubert, C., 2005. Characterization of isomeric allylic diols resulting from chlorophyll phytyl side chain photo- and autoxidation by electron ionization gas chromatography/mass spectrometry. *Rapid Communications in Mass Spectrometry* 19, 637-646.
- Rontani, J.-F., Zabeti, N., Wakeham, S.G., 2009. The fate of marine lipids: Biotic vs. abiotic degradation of particulate sterols and alkenones in the Northwestern Mediterranean Sea. *Marine Chemistry* 113, 9-18.

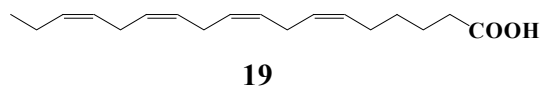
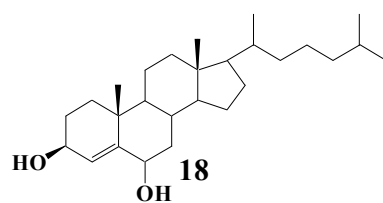
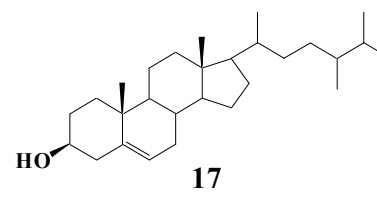
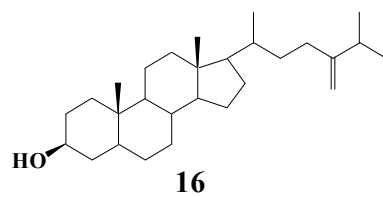
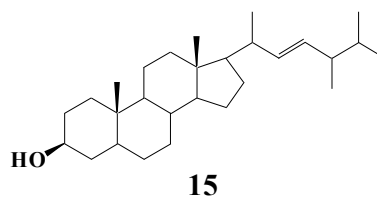
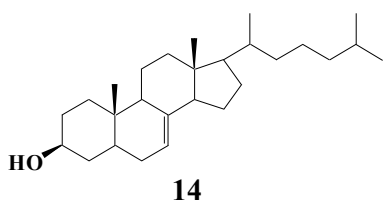
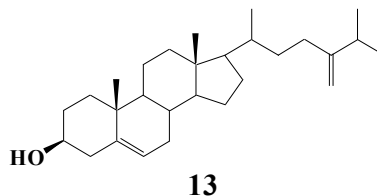
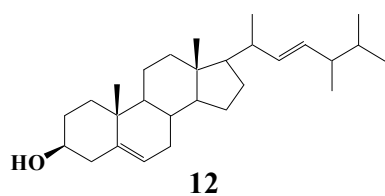
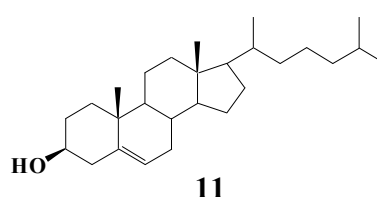
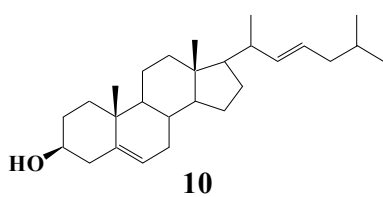
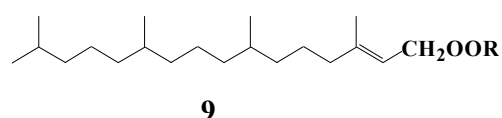
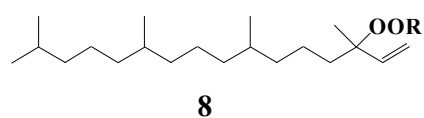
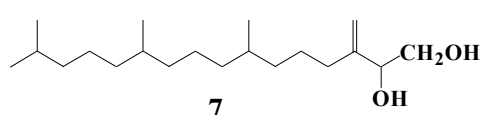
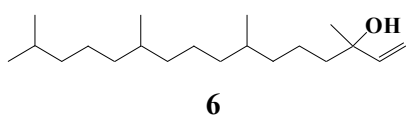
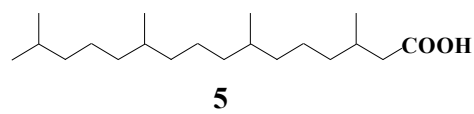
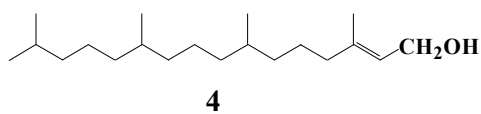
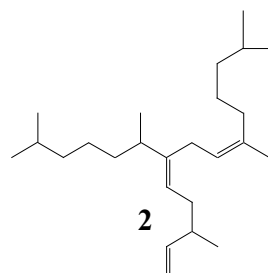
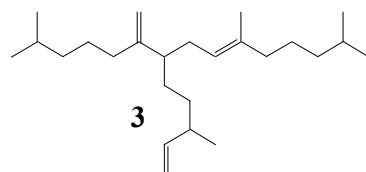
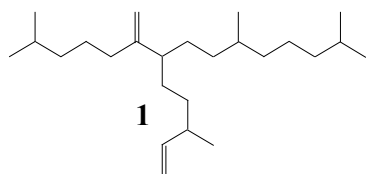
- Rontani, J.-F., Belt, S.T., Vaultier, F., Brown, T.A., 2011. Visible light-induced photo-oxidation of highly branched isoprenoid (HBI) alkenes: a significant dependence on the number and nature of the double bonds. *Organic Geochemistry* 42, 812-822.
- Rontani, J.-F., 2012. Photo- and free radical-mediated oxidation of lipid components during the senescence of phototrophic organisms. In: T. Nagata Ed., *Senescence*. Intech, Rijeka, pp. 3-31.
- Rontani, J.-F., Charriere, B., Forest, A., Heussner, S., Vaultier, F., Petit, M., Delsaut, N., Fortier, L., Sempéré, R., 2012. Intense photooxidative degradation of planktonic and bacterial lipids in sinking particles collected with sediment traps across the Canadian Beaufort Shelf (Arctic Ocean). *Biogeosciences* 9, 4787-4802.
- Rontani, J.-F., Charrière, B., Sempéré, R., Doxaran, D., Vaultier, F., Vonk, J.E., Volkman, J.K., 2014a. Degradation of sterols and terrigenous organic matter in waters of the Mackenzie Shelf, Canadian Arctic. *Organic Geochemistry* 75, 61-73.
- Rontani, J.-F., Belt, S., Vaultier, F., Brown, T., Massé, G., 2014b. Autoxidative and photooxidative reactivity of highly branched isoprenoid (HBI) alkenes. *Lipids*, 49(5), 481-494.
- Rontani, J.-F., Galeron, M.-A., 2016. Autoxidation of chlorophyll phytyl side-chain in senescent phototrophic organisms: a potential source of isophytol in the environment. *Organic Geochemistry* 97, 37-40.
- Rontani, J.-F., Amiraux, R., Lalande, C., Babin, M., Kim, H.-R., Belt, S.T., 2018. Use of palmitoleic acid and its oxidation products for monitoring the degradation of ice algae in Arctic waters and bottom sediments. *Organic Geochemistry* 124, 88-102.
- Rossi, S., Sabates, A., Latasa, M., reyes, E., 2006. Lipid biomarkers and trophic linkages between phytoplankton, zooplankton and anchovy (*Engraulis encrasicolus*) larvae in the NW Mediterranean. *Journal of Plankton Research* 28, 551-562.

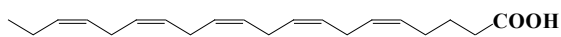
- Sakshaug, E., Johnsen, G., Kristiansen, S., von Quillfeldt, C., Rey, F., Slagstad, D., Thingstad, F., 2009. Phytoplankton and primary production. In: Sakshaug, E., Johnsen, G., Kovacs, K. (Eds), *Ecosystem Barents Sea*. Tapir Academic Press, Trondheim, pp.167–208.
- Scherer, R.P., 1994. A new method for the determination of absolute abundance of diatoms and other silt-sized sedimentary particles. *Journal of Paleolimnology* 12 (1), 171–178.
- Schmidt, K., Brown, T.A., Belt, S.T., Ireland, L.C., Taylor, K.W.R., Thorpe, S.E., Ward, P., Atkinson, A., 2018. Do pelagic grazers benefit from sea ice? Insights from the Antarctic sea ice proxy IPSO₂₅. *Biogeosciences* 15, 1987– 2006.
- Schrader, H.J., Gersonde, R., 1978. Diatoms and silicoflagellates. In: Zachariasse, A. (Ed.), *Micropaleontological Counting Methods and Techniques - An Exercise on Eight Meters Section of the Lower Pliocene of Capo Rossello, Sicily*. Utrecht Micropaleontology Bulletin, 17, pp. 129–176.
- Scott, F., Marchant, H.J., 2005. *Antarctic Marine Protists* 1st ed. F. Scott and H. J. Marchant, eds., Canberra, Hobart: Australian Biological Resources Study and Australian Antarctic Division.
- Serreze, M.C., Stroeve, J., Barrett, A.P., Boisvert, L.N., 2016. Summer atmospheric circulation anomalies over the Arctic Ocean and their influence on September sea ice extent. A cautionary tale. *Journal of Geophysical Research: Atmospheres* 121, 11463–11485.
- Smik, L., Belt, S.T., Lieser, J.L., Armand, L.K., Leventer, A., 2016. Distributions of highly branched isoprenoid alkenes and other algal lipids in surface waters from East Antarctica: Further insights for biomarker-based paleo sea-ice reconstruction. *Organic Geochemistry* 95, 71–80.
- Smith, L.L., 1981. *The autoxidation of cholesterol*. Plenum Press, New York, pp. 119-132.

- Smith, R.I.L., 1994. Vascular plants as bioindicators of regional warming in Antarctica. *Oecologia* 99, 322-328.
- Smith, W.O., 1987. Phytoplankton dynamics in marginal ice zones. *Oceanography and Marine Biology* 25, 11-38.
- Smith, W.O., Jr., Nelson, D.M., 1986. The importance of ice-edge blooms in the Southern Ocean. *Biosciences* 36, 251-257.
- Stroeve, J.C., Serreze, M.C., Holland, M.M., Kay, J.E., Malanik, J., Barrett, A.P., 2012. The Arctic's rapidly shrinking sea ice cover: a research synthesis. *Climate Change* 110, 1005-1027.
- Thomas, D.N., 2017. Sea ice 3rd ed. Wiley-Blackwell: pp 664.
- Tomas, C.R., 1997. Identifying marine phytoplankton, San Diego: Academic Press.
- Utermöhl, H., 1958. Zur Vervollkommnung der quantitativen Phytoplankton-Methodik. *Internationale Vereinigung für theoretische und angewandte Limnologie: Mitteilungen* 9, 1-38.
- Volkman, J.K., Corner, E.D.S., Eglinton, G., 1980. Transformations of biolipids in the marine food web and in underlying bottom sediments, *Colloque International du Centre National de la Recherche Scientifique* 293, 185-197.
- Volkman, J.K., 1986. A review of sterol markers for marine and terrigenous organic matter. *Organic Geochemistry* 9, 83-99.
- Volkman, J.K., 2003. Sterols in microorganisms. *Applied Microbiology and Biotechnology* 60, 495-506.
- Walsh, J.E., Fetterer, F., Scott Stewart, J., Chapman, W.L., 2017. A database for depicting Arctic sea ice variations back to 1850. *Geographical Review* 107, 89-107.
- Wakeham, S.G., 1989. Reduction of stenols to stanols in particulate matter at oxic-anoxic boundaries in seawater. *Nature* 342, 787-790.

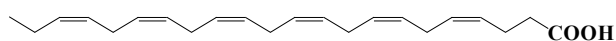
889 Yin, H., Xu, L., Porter, N.A., 2011. Free radical lipid peroxidation: mechanisms and
890 analysis. Chemical Review 111, 5944-5972.
891

APPENDIX

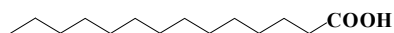




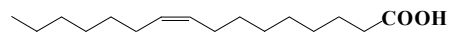
20



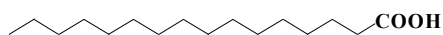
21



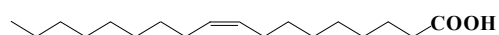
22



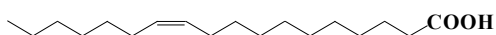
23



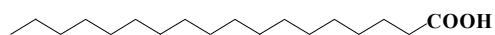
24



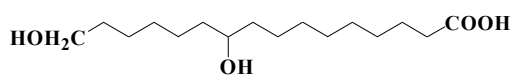
25



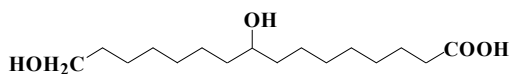
26



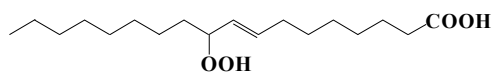
27



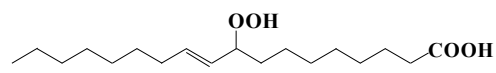
28



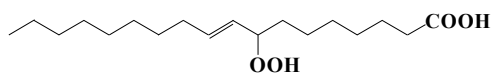
29



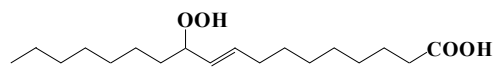
30



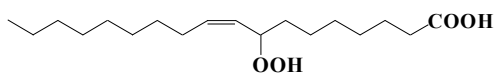
31



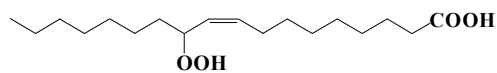
32



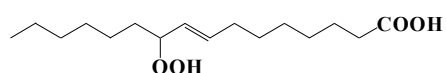
33



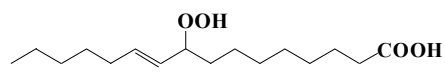
34



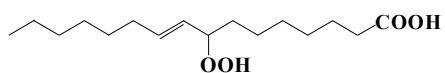
35



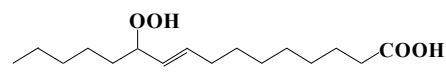
36



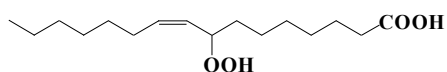
37



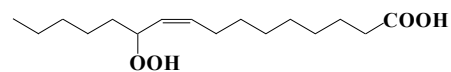
38



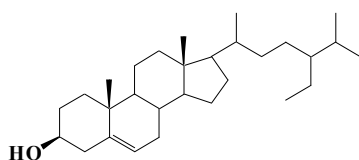
39



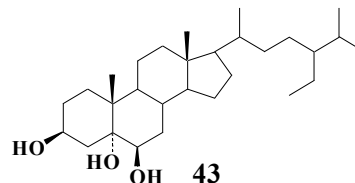
40



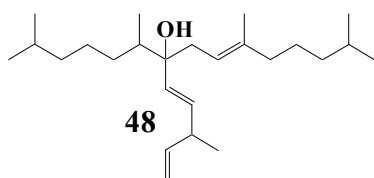
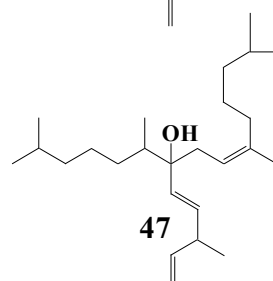
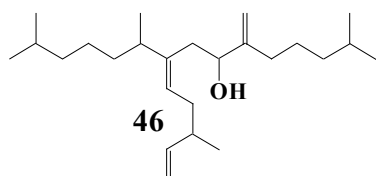
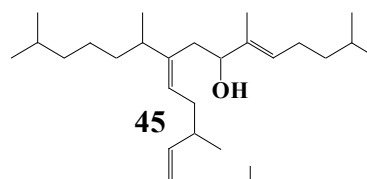
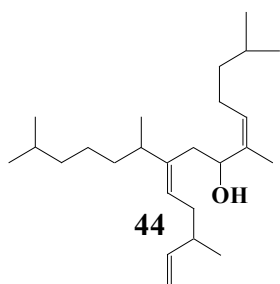
41



42



43



894

FIGURE CAPTIONS

Figure 1. Summary map showing sampling locations (CB = Commonwealth Bay).

Figure 2. Proposed pathways for autoxidation of chlorophyll phytyl side chain.

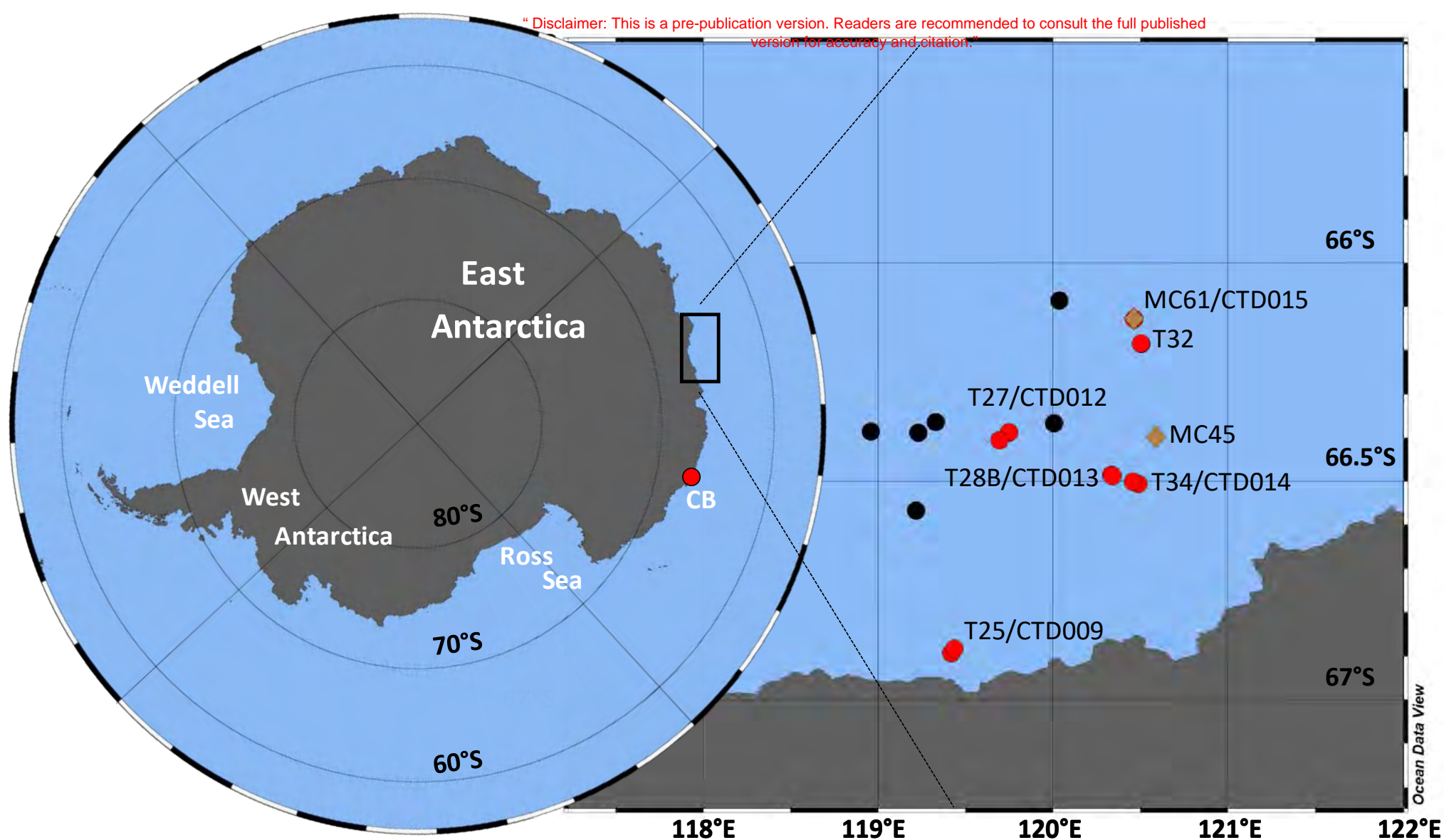
Figure 3. Photooxidation percentages of *epi*-brassicasterol (**12**), 24-methylencholesterol (**13**) and chlorophyll in the CTD samples collected at the stations selected for lipid oxidation product analyses. The very low photooxidation percentages of sterols in the samples collected at the station 32 were not included in this figure.

Figure 4. Photo- and autoxidation percentages of palmitoleic (**23**) and oleic (**25**) acids in the CTD samples collected at the stations selected for lipid oxidation product analyses. The weak oxidation percentages of palmitoleic acid in the samples collected at the station 32 are given in Table 3.

Figure 5. MRM chromatograms (m/z 213 \rightarrow 117, m/z 213 \rightarrow 123 and m/z 213 \rightarrow 157) for standard oxidation products of the HBI triene **2** (A) and CB phytoplanktonic sample collected in Commonwealth Bay (B).

Figure 6. MRM chromatograms (m/z 295 \rightarrow 93, m/z 295 \rightarrow 107 and m/z 295 \rightarrow 183) for standard oxidation products of the HBI triene **2** (A) and CB phytoplanktonic sample collected from Commonwealth Bay (B).

Figure 7. Conceptual scheme summarizing sedimentation and degradation of ice algae and open water phytoplankton in east Antarctica. Note that in some cases the increase of the ratio IPSO₂₅(**1**)/HBI III (**2**) with depth may be due to the faster sedimentation rate of aggregated sympagic algae relative to open water phytoplankton and in other cases to an intense photooxidation (in the euphotic layer) or autooxidation (in the entire water column and in the oxic layer of sediments) of the HBI triene **2**.



- Detailed lipid analysis (oxidation products)
- Other CTD stations (native lipids only)
- ◆ Sediments (Megacores)

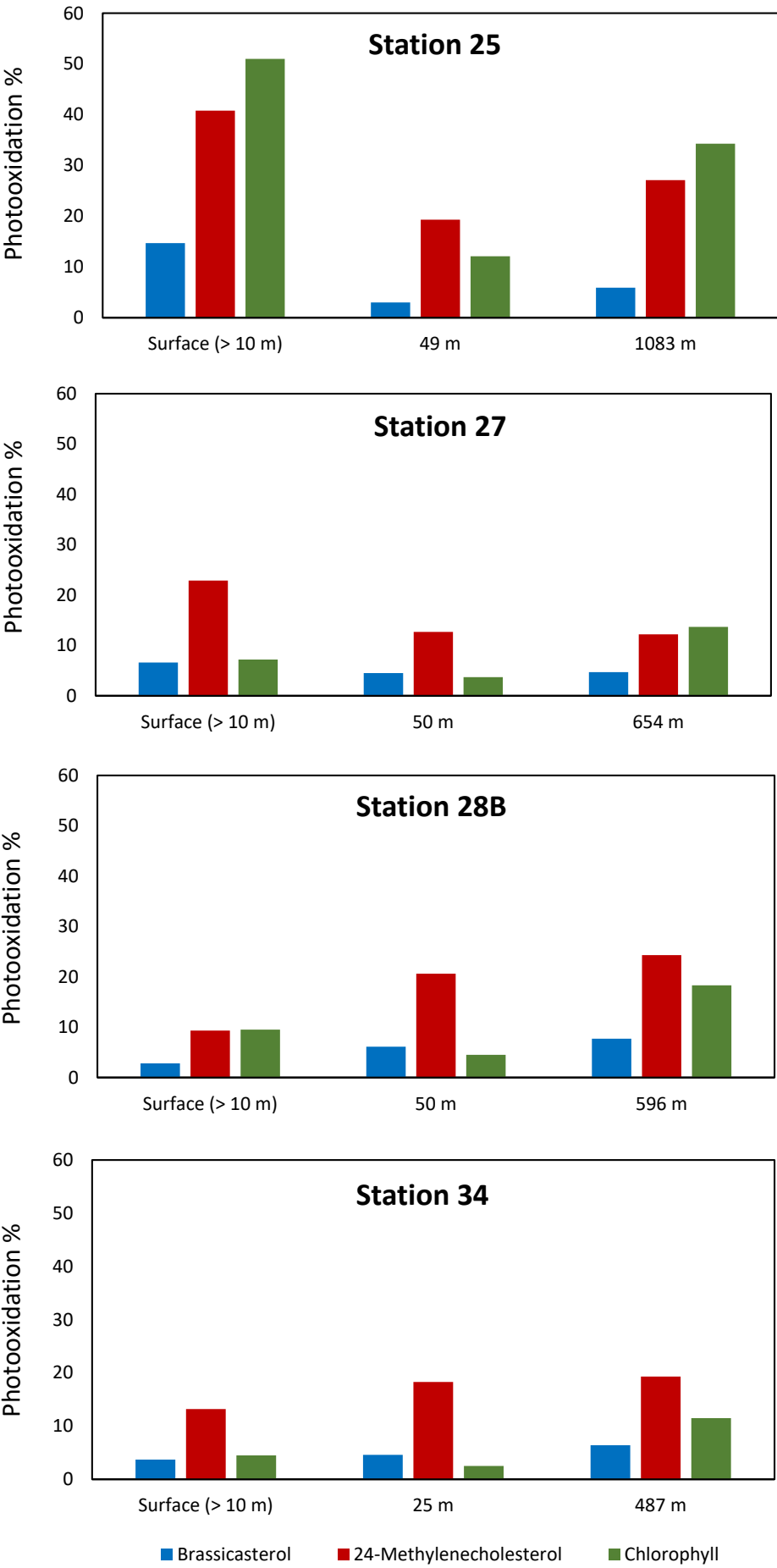
The reaction scheme illustrates the synthesis of allylic alcohols **4** and **6** from an allylic ester and a ketone.

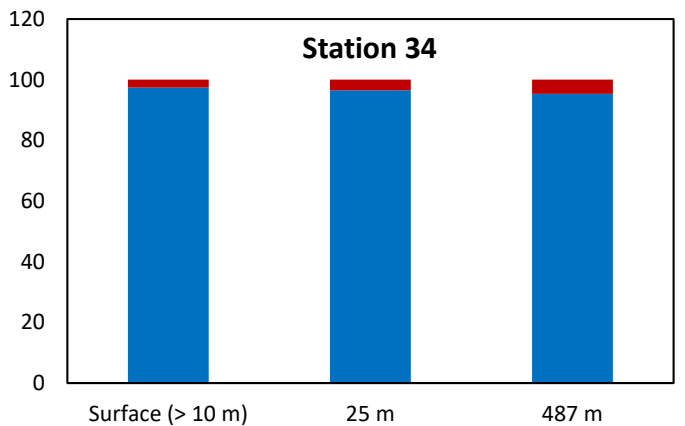
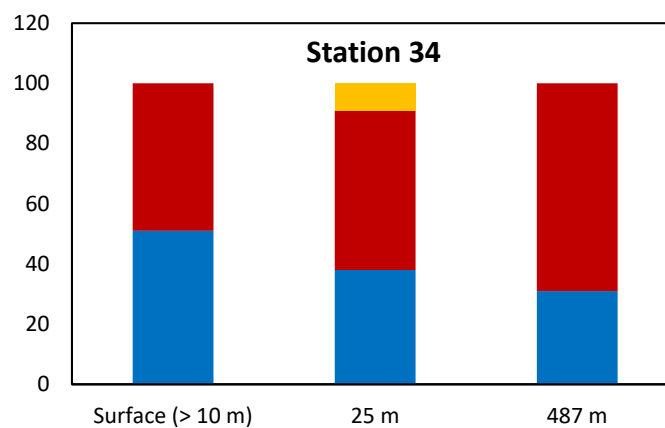
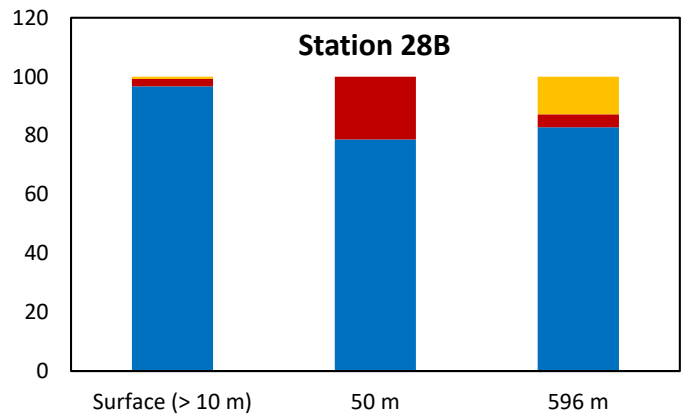
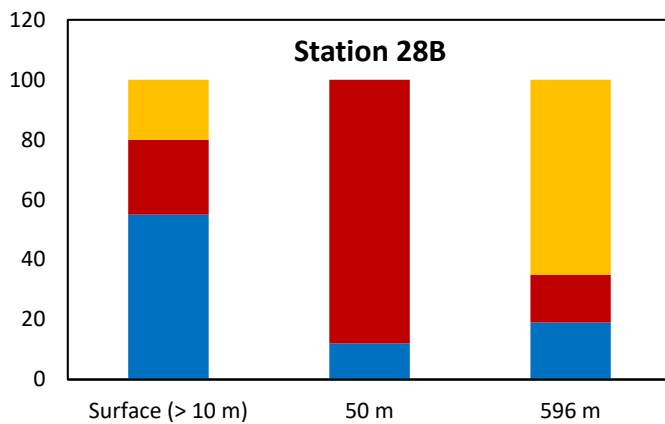
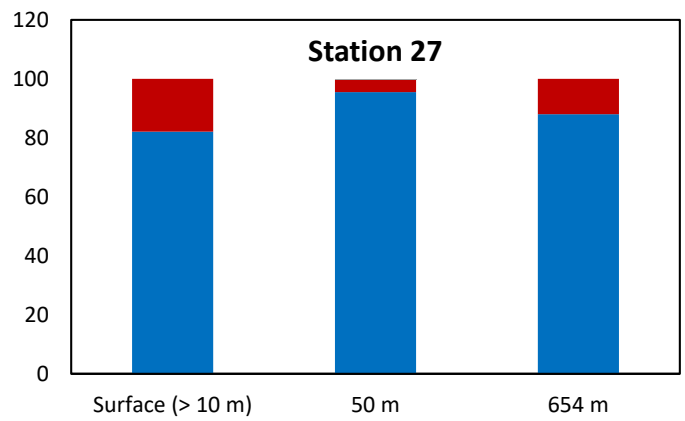
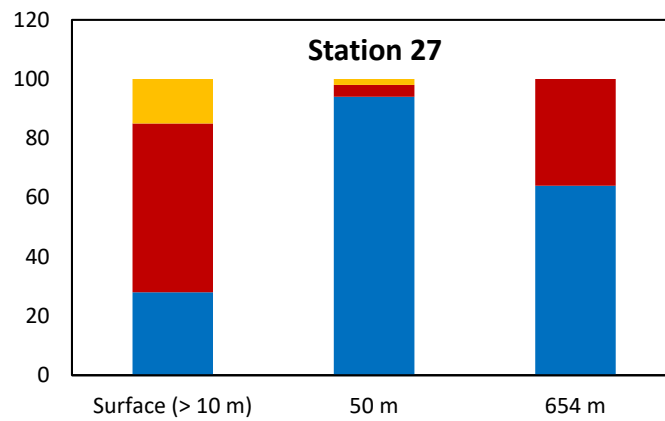
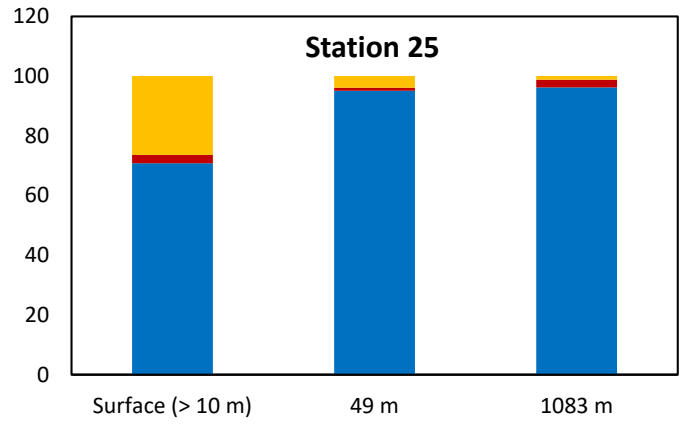
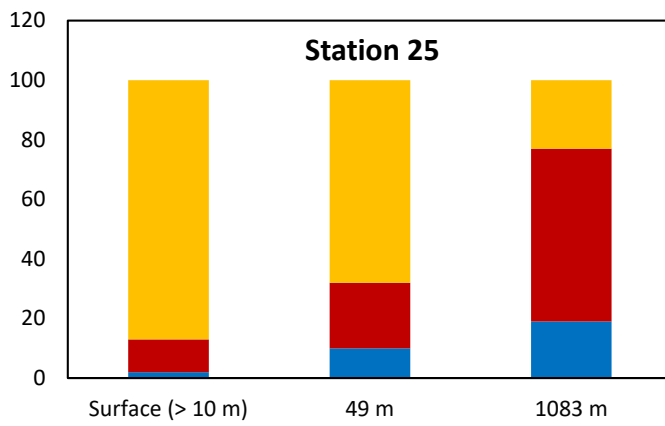
Top Pathway:

- Allylation:** An allylic ester (with an ROO^\bullet group) reacts with a ketone ($\text{O}=\text{C}-\text{R}_2$) to form an allylic ether intermediate (**8**) and a radical species ($\text{O}^\bullet=\text{C}-\text{R}_2$).
- Radical Interconversion:** Intermediate **8** is in equilibrium with a radical species ($\text{R}_1\text{C}(\text{OO}^\bullet)\text{CH}=\text{CH}_2$) via $+\text{R}^\bullet$ and $-\text{R}^\bullet$ steps.
- Allylic rearrangement:** The radical species undergoes allylic rearrangement to form an allylic radical ($\text{R}_1\text{CH}^\bullet\text{CH}=\text{CH}_2$).
- NaBH₄ reduction:** The allylic radical is reduced by NaBH_4 to form the allylic alcohol **6** ($\text{R}_1\text{CH}(\text{OH})\text{CH}=\text{CH}_2$).

Bottom Pathway:

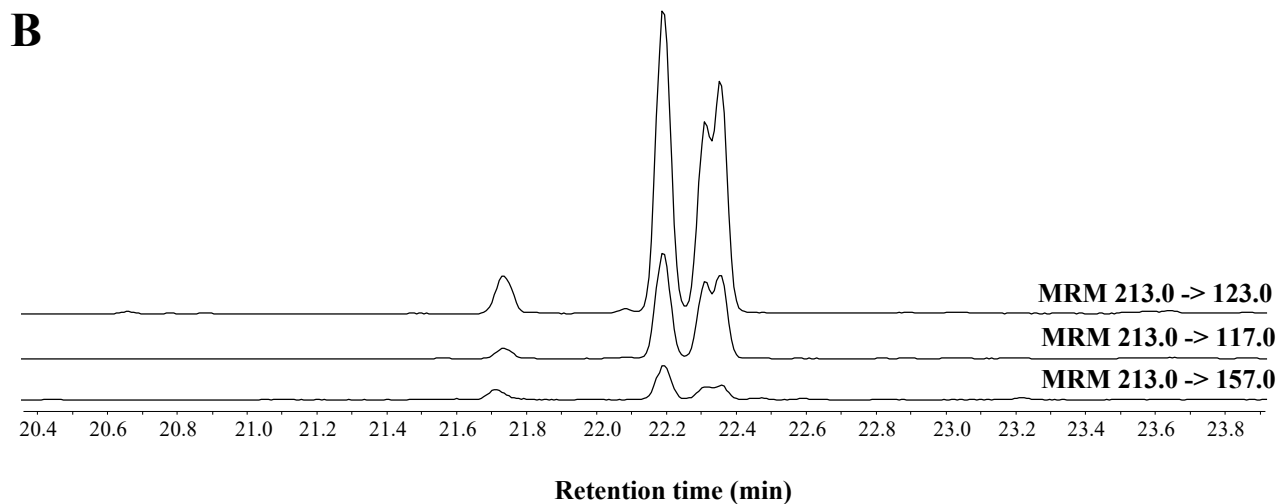
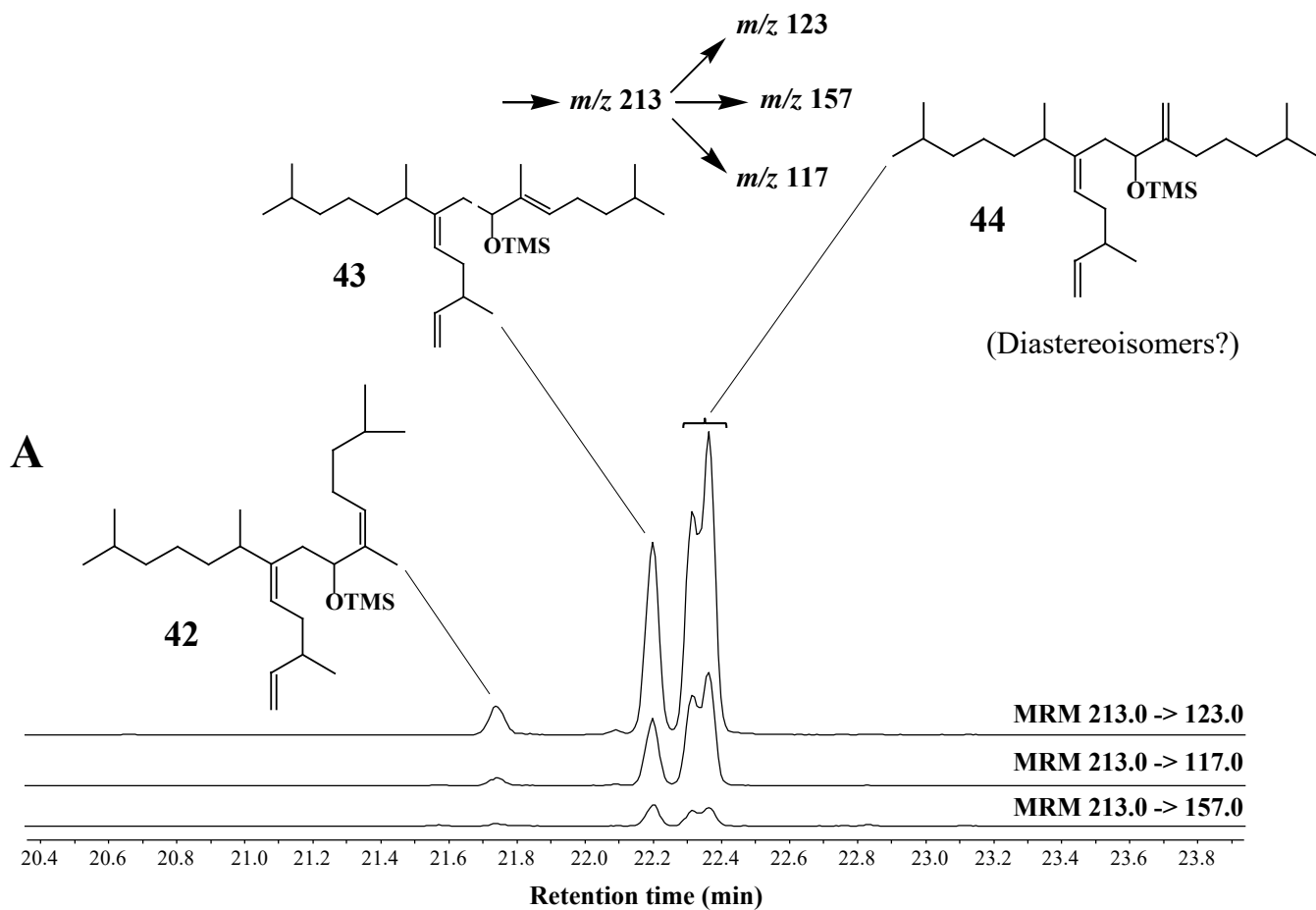
- Allylic rearrangement:** The allylic ester (with an $\text{CH}_2\text{OO}^\bullet$ group) undergoes allylic rearrangement to form an allylic radical ($\text{R}_1\text{CH}^\bullet\text{CH}=\text{CH}_2$).
- Radical Interconversion:** The allylic radical is in equilibrium with a radical species ($\text{R}_1\text{C}(\text{OO}^\bullet)\text{CH}=\text{CH}_2$) via $+\text{R}^\bullet$ and $-\text{R}^\bullet$ steps.
- NaBH₄ reduction:** The radical species is reduced by NaBH_4 to form the allylic alcohol **4** ($\text{R}_1\text{CH}(\text{OH})\text{CH}=\text{CH}_2$).

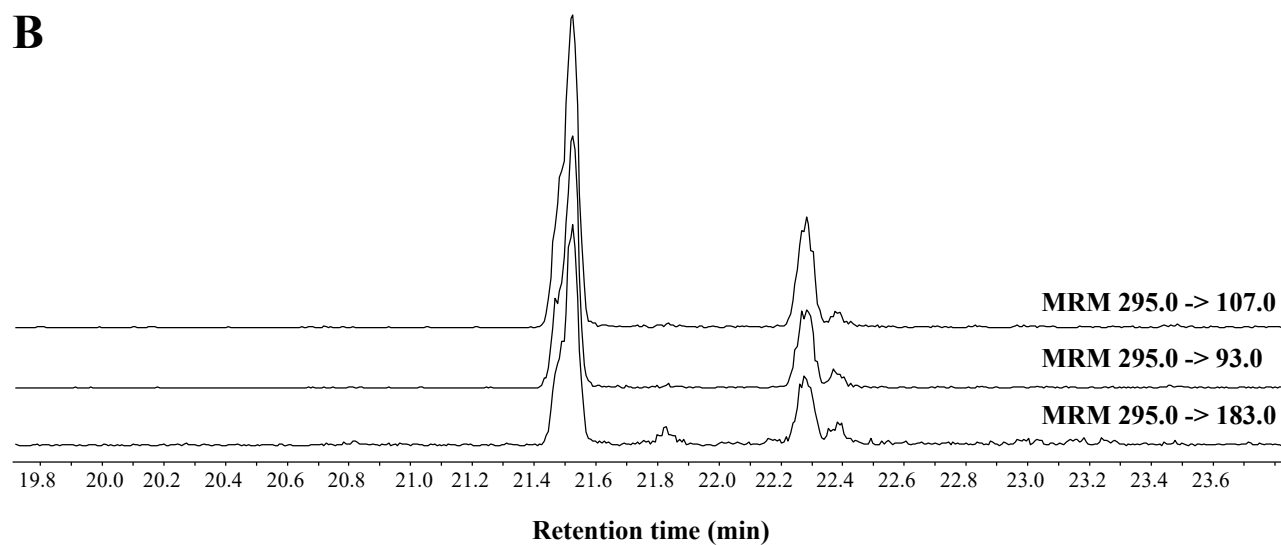
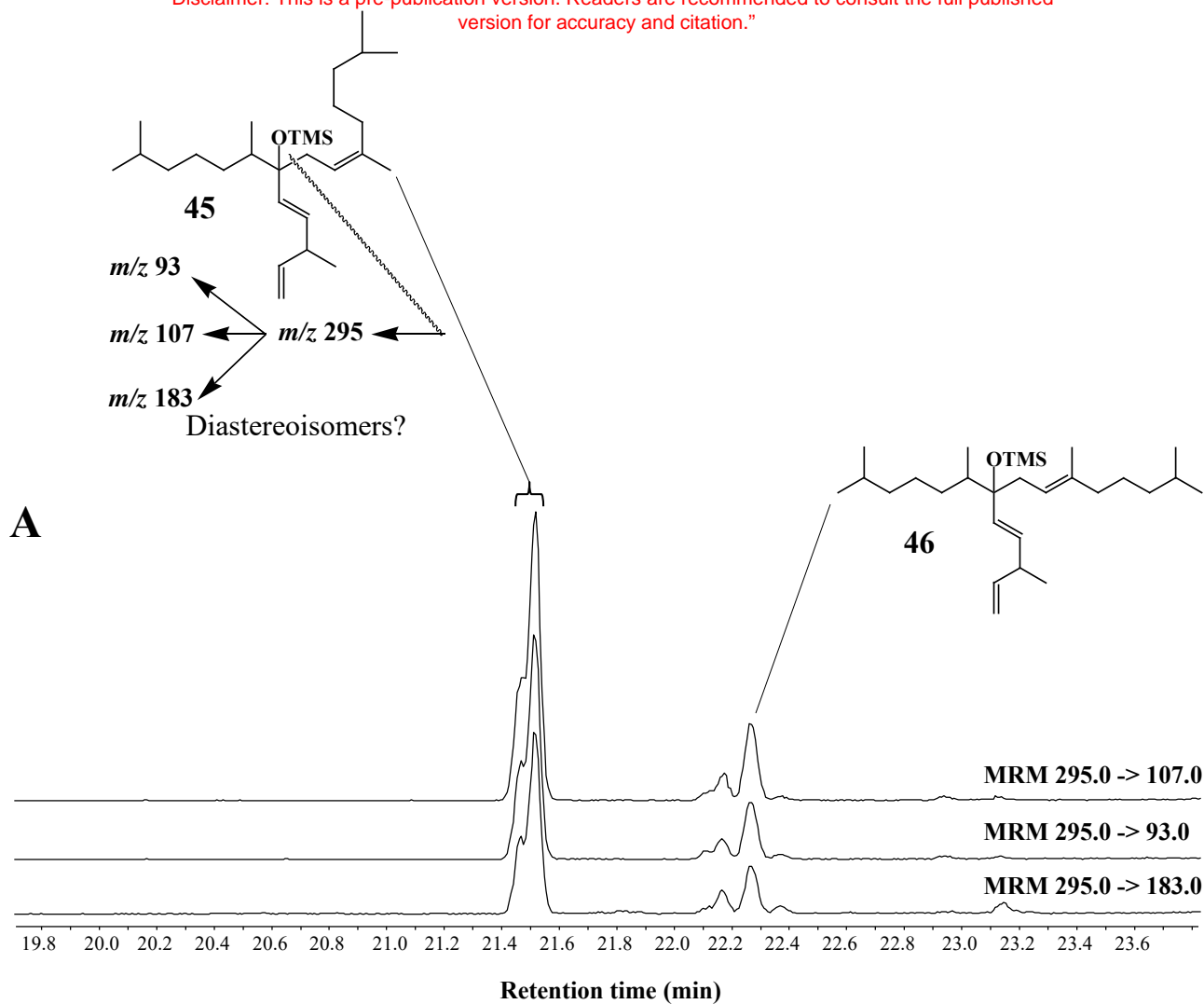


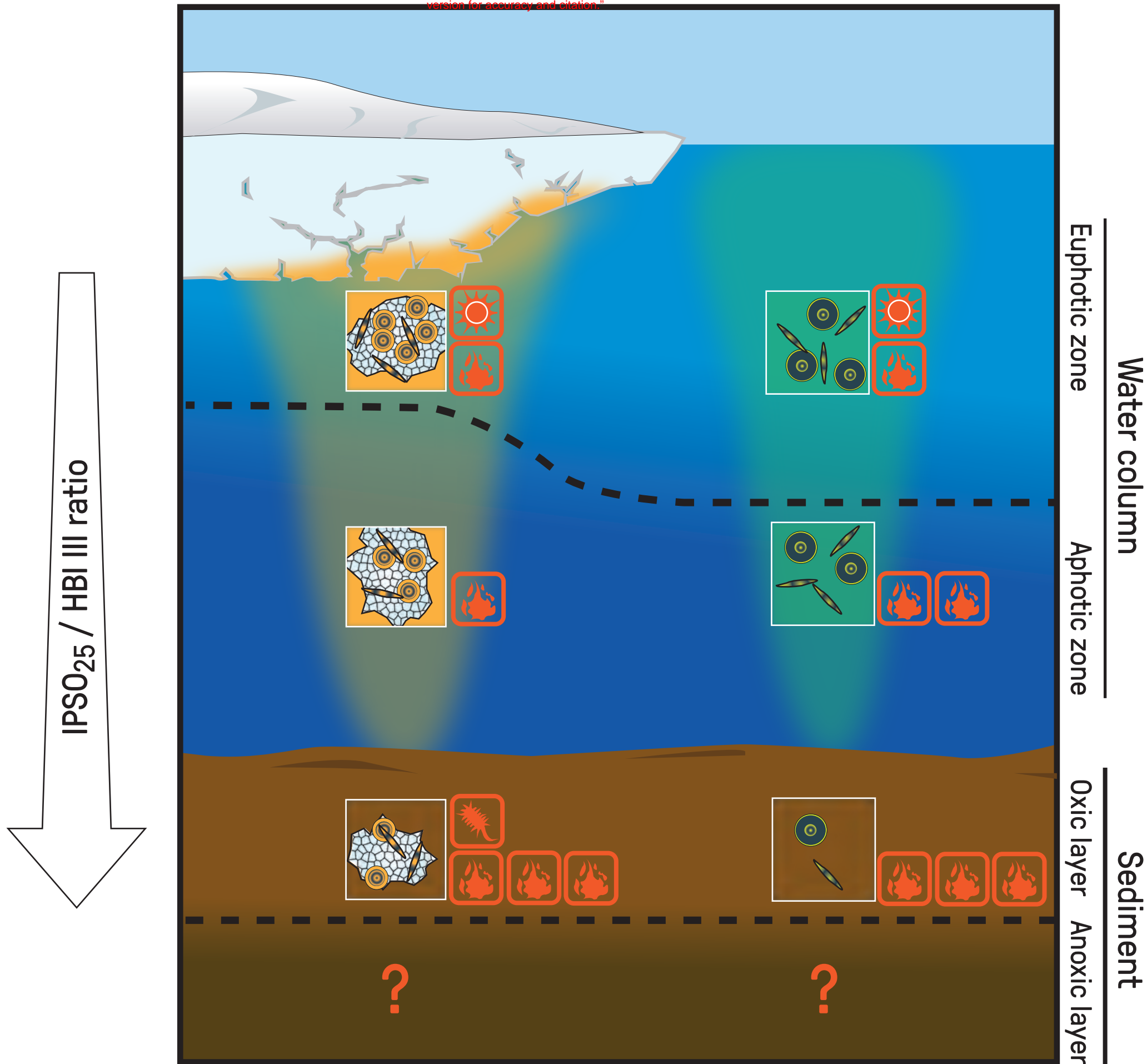


Palmitoleic acid Autoxidation Photooxidation

Oleic acid Autoxidation Photooxidation







Extracellular polymeric substances
Sympagic algae Phytoplankton

Degradation pathways:

Photooxidation Autooxidation Bacterial

Table 1

Different indicators measured at the five stations selected for lipid degradation analyses.

Station	Depth (m)	IPSO ₂₅ (1)/ HBI triene (2)	Cuticular waxes ^a / palmitic acid (24)	<i>Epi</i> -brassicastanol (12)/ <i>epi</i> -brassicasterol (16)	(Palmitoleic acid (23)+ ox ^b)/ palmitic acid (24)	Isophytol (6)/ phytol (4)
25	10<	0.21	0	0.24	30.91	0.45
25	49	0.26	0	0.20	3.42	1.64
25	1083	2.57	0	0.32	1.65	0.60
27	10<	0.26	0.07	0.17	1.82	0
27	50	0.14	2.15	0.21	0.42	0.01
27	654	1.74	0	0.29	0.25	0.08
28B	10<	0.51	0.02	0.14	1.01	0.30
28B	50	0.44	0.03	0.24	3.11	0.06
28B	596	1.61	0	0.16	4.02	0.20
32	10<	0.21	0	0.10	0.05	0.13
32	40	0.37	0	0.09	0.08	0.08
32	563	0.88	0	0.17	0.02	0.07
34	10<	0.25	0.04	0.14	1.11	0.04
34	25	0.21	1.23	0.17	1.10	0.05
34	487	1.54	0	0.28	1.36	0.03

^a Mixtures of 9,16-dihydroxyhexadecanoic (**29**) and 10,16-dihydroxyhexadecanoic (**28**) acids

^b Photo- and autoxidation products

Table 2

Comparison of the ratio **1/2** and the autoxidation state of some other algal lipids in SPM and underlying sediments. See Fig. 1 for sample locations.

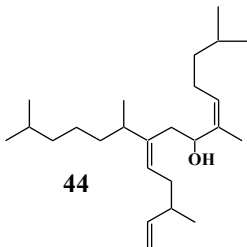
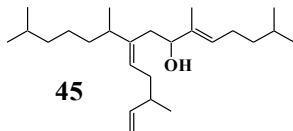
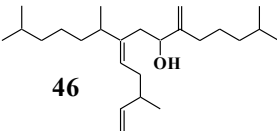
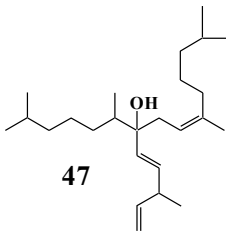
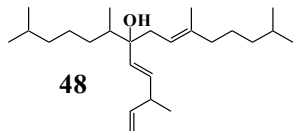
Station – sample type	Depth (m)	IPSO ₂₅ (1)/ HBI triene (2)	Sitosterol (42) autoxidation %	Palmitoleic acid (23) autoxidation %	(<i>F. curta</i> + <i>F. cylindrus</i>) / <i>F. kerguelensis</i>
T32 – SPM	10<	0.2	0	1.3	20.6
CTD015 – SPM	40	0.4	0	9.3	18.8
CTD015 – SPM	563	0.9	0	21.8	8.0
MC61 – overlying water	579	1.6	*	*	0.5
MC61 – diatomaceous ‘fluff’	579	2.6	*	*	N/A
MC61 – sediment (1–2 cm)	579	7.5	28.4	53.4	0.7
MC45 – sediment (1–2 cm)	538	11.3	46.3	51.6	0.8

* - not measured

N/A - abundances too low

Table 3

Percentage^a of oxidation products of HBI triene (**2**) detected after NaBH₄-reduction of filtered phytoplankton from Commonwealth Bay (East Antarctica)

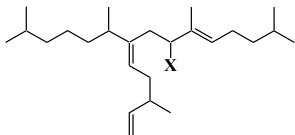
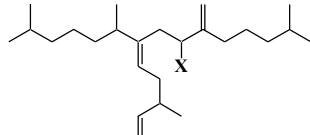
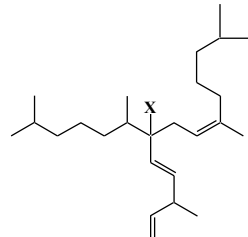
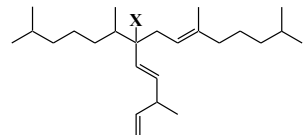
Sample	 44	 45	 46	 47	 48
CB	0.6	9.1	11.2	10.2	5.1
AS607	^b	53.4	71.2	65.1	52.7
AS608	10.4	43.6	96.4	9.1	32.7

^a Relative to the residual parent HBI

^b Coelution problem

Table 4

Relative percentages of intact hydroperoxides and their ketonic and alcoholic degradation products measured in the case of the main HBI oxidation products present in phytoplankton from Commonwealth Bay (East Antarctica) (CB sample).

X-				
HO-	18	22	21	45
O=	1	3	-	-
HOO-	81	75	79	55

Supplementary Table 1

Sample ID	Latitude	Longitude	Collection Date (2014)	Water depth (m)	IPSO ₂₅ (pg mL ⁻¹)	HBI III (pg mL ⁻¹)	IPSO ₂₅ /HBI III	Epi-brassicasterol (pg mL ⁻¹)	24-Methylencholesterol (pg mL ⁻¹)	22-Dehydrocholesterol (pg mL ⁻¹)	Cholesterol (pg mL ⁻¹)	22-dihydrocondrillasterol (pg mL ⁻¹)
surface												
T-25	-66.883	119.437	20/02	<10	0.215	1.039	0.21	690	112	1033	319	241
T-27	-66.406	119.694	25/02	<10	0.180	0.698	0.26	236	47	352	190	82
T-28B	-66.488	120.340	25/02	<10	0.371	0.724	0.51	275	52	246	171	97
T-32	-66.184	120.503	05/03	<10	0.246	1.160	0.25	249	49	264	155	115
T-34	-66.501	120.457	06/03	<10	0.347	1.414	0.21	220	42	196	166	120
CTD-002	-66.086	120.037	10/02	1	0.317	0.600	0.53	248	59	325	192	49
CTD-004	-66.367	120.006	12/02	0	0.105	0.395	0.27	525	80	983	370	227
CTD-005	-66.364	119.331	17/02	10	0.099	0.288	0.35	277	45	326	204	55
CTD-006	-66.389	119.231	17/02	10	0.302	1.669	0.18	437	72	542	270	205
CTD-007	-66.386	118.960	17/02	10	0.188	0.415	0.45	279	55	456	125	31
CTD-008	-66.567	119.217	18/02	9	0.112	0.441	0.25	467	66	509	280	125
CTD-009	-66.893	119.418	20/02	7	0.151	0.705	0.21	664	94	1135	397	224
CTD-010	-66.185	120.504	21/02	5	0.195	1.056	0.18	270	56	375	191	779
CTD-012	-66.388	119.749	25/02	5	0.351	1.143	0.31	336	62	527	207	134
CTD-013	-66.485	120.333	25/02	5	0.147	0.690	0.21	265	46	340	225	134
CTD-014	-66.506	120.487	06/03	5	0.156	0.523	0.30	221	33	212	183	107
CTD-015	-66.129	120.464	06/03	5	0.141	0.965	0.15	266	57	270	194	200
Mean							0.28					

Sample ID	Latitude	Longitude	Collection Date (2014)	Water depth (m)	C ₁₄ FA (pg mL ⁻¹)	C ₁₆ FA (pg mL ⁻¹)	C _{16:1ω7} FA (pg mL ⁻¹)	C ₁₈ FA (pg mL ⁻¹)
surface								
T-25	-66.883	119.437	20/02	<10	2432	2624	1622	277
T-27	-66.406	119.694	25/02	<10	852	1258	637	244
T-28B	-66.488	120.340	25/02	<10	923	1287	720	218
T-32	-66.184	120.503	05/03	<10	697	971	502	169
T-34	-66.501	120.457	06/03	<10	884	1216	688	214
CTD-002	-66.086	120.037	10/02	1	1071	1624	661	357
CTD-004	-66.367	120.006	12/02	0	520	1510	797	381
CTD-005	-66.364	119.331	17/02	10	549	1610	259	596
CTD-006	-66.389	119.231	17/02	10	2394	2853	1452	296
CTD-007	-66.386	118.960	17/02	10	279	674	312	154
CTD-008	-66.567	119.217	18/02	9	1968	2474	1279	157
CTD-009	-66.893	119.418	20/02	7	2509	3367	1412	541
CTD-010	-66.185	120.504	21/02	5	786	1331	539	339
CTD-012	-66.388	119.749	25/02	5	1647	1904	882	207
CTD-013	-66.485	120.333	25/02	5	1021	1588	650	349
CTD-014	-66.506	120.487	06/03	5	1117	1594	649	327
CTD-015	-66.129	120.464	06/03	5	850	1357	521	284

Supplementary Table 1

Sample ID	Latitude	Longitude	Collection Date (2014)	Water depth (m)	IPSO ₂₅ (pg mL ⁻¹)	HBI III (pg mL ⁻¹)	IPSO ₂₅ /HBI III	Epi-brassicasterol (pg mL ⁻¹)	24-Methylencholesterol (pg mL ⁻¹)	22-Dehydrocholesterol (pg mL ⁻¹)	Cholesterol (pg mL ⁻¹)	22-dihydrocondrillasterol (pg mL ⁻¹)
sub-surface												
CTD-002	-66.086	120.037	10/02	20	0.187	0.245	0.77	82	9	97	63	12
CTD-004	-66.367	120.006	12/02	60	0.279	1.103	0.25	326	62	624	156	117
CTD-005	-66.364	119.331	17/02	60	0.296	0.671	0.44	119	20	157	94	33
CTD-006	-66.389	119.231	17/02	40	0.321	1.564	0.21	289	66	336	228	88
CTD-007	-66.386	118.960	17/02	25	0.346	0.757	0.46	506	76	801	259	35
CTD-008	-66.567	119.217	18/02	50	0.126	0.268	0.47	140	18	221	67	10
CTD-009	-66.893	119.418	20/02	60	0.194	0.750	0.26	233	30	307	102	95
CTD-010	-66.185	120.504	21/02	35	0.311	1.297	0.24	111	18	137	87	36
CTD-012	-66.388	119.749	25/02	50	0.288	2.021	0.14	203	37	331	136	80
CTD-013	-66.485	120.333	25/02	50	0.588	1.348	0.44	137	30	165	120	65
CTD-014	-66.506	120.487	06/03	25	0.257	1.250	0.21	145	26	125	98	88
CTD-015	-66.129	120.464	06/03	40	0.440	1.181	0.37	125	24	102	82	87
Mean							0.36					

Sample ID	Latitude	Longitude	Collection Date (2014)	Water depth (m)	C ₁₄ FA (pg mL ⁻¹)	C ₁₆ FA (pg mL ⁻¹)	C _{16:1ω7} FA (pg mL ⁻¹)	C ₁₈ FA (pg mL ⁻¹)
sub-surface								
CTD-002	-66.086	120.037	10/02	20	394	899	205	366
CTD-004	-66.367	120.006	12/02	60	658	1599	592	415
CTD-005	-66.364	119.331	17/02	60	841	1384	462	329
CTD-006	-66.389	119.231	17/02	40	1542	2463	908	501
CTD-007	-66.386	118.960	17/02	25	512	1399	593	369
CTD-008	-66.567	119.217	18/02	50	522	1089	255	242
CTD-009	-66.893	119.418	20/02	60	1379	2060	704	507
CTD-010	-66.185	120.504	21/02	35	700	1329	384	267
CTD-012	-66.388	119.749	25/02	50	1188	1756	667	280
CTD-013	-66.485	120.333	25/02	50	1067	1754	656	442
CTD-014	-66.506	120.487	06/03	25	956	1411	596	334
CTD-015	-66.129	120.464	06/03	40	981	1366	601	195

Supplementary Table 1

Sample ID	Latitude	Longitude	Collection Date (2014)	Water depth (m)	IPSO ₂₅ (pg mL ⁻¹)	HBI III (pg mL ⁻¹)	IPSO ₂₅ /HBI III	Epi-brassicasterol (pg mL ⁻¹)	24-Methylencholesterol (pg mL ⁻¹)	22-Dehydrocholesterol (pg mL ⁻¹)	Cholesterol (pg mL ⁻¹)	22-dihydrocondrillasterol (pg mL ⁻¹)
deep												
CTD-002	-66.086	120.037	10/02	480	0.086	0.042	2.02	24	2	18	30	8
CTD-004	-66.367	120.006	12/02	610	0.157	0.067	2.36	52	10	61	50	6
CTD-005	-66.364	119.331	17/02	830	0.061	0.017	3.49	22	5	24	56	LOD
CTD-006	-66.389	119.231	17/02	860	0.080	0.028	2.87	28	5	26	34	LOD
CTD-007	-66.386	118.960	17/02	890	0.121	0.028	4.31	30	4	20	26	LOD
CTD-008	-66.567	119.217	18/02	670	0.092	0.043	2.13	36	6	42	47	LOD
CTD-009	-66.893	119.418	20/02	1080	0.128	0.050	2.57	104	20	110	73	LOD
CTD-010	-66.185	120.504	21/02	530	0.169	0.146	1.16	44	5	42	37	2
CTD-012	-66.388	119.749	25/02	650	0.105	0.060	1.74	62	11	81	83	LOQ
CTD-013	-66.485	120.333	25/02	600	0.126	0.078	1.61	66	8	94	319	7
CTD-014	-66.506	120.487	06/03	490	0.086	0.056	1.54	25	8	42	43	LOQ
CTD-015	-66.129	120.464	06/03	560	0.127	0.144	0.88	39	6	34	112	15
Mean							2.22					

Sample ID	Latitude	Longitude	Collection Date (2014)	Water depth (m)	C ₁₄ FA (pg mL ⁻¹)	C ₁₆ FA (pg mL ⁻¹)	C _{16:1ω7} FA (pg mL ⁻¹)	C ₁₈ FA (pg mL ⁻¹)
deep								
CTD-002	-66.086	120.037	10/02	480	104	373	55	226
CTD-004	-66.367	120.006	12/02	610	100	694	98	566
CTD-005	-66.364	119.331	17/02	830	121	678	111	432
CTD-006	-66.389	119.231	17/02	860	154	503	102	231
CTD-007	-66.386	118.960	17/02	890	117	357	85	140
CTD-008	-66.567	119.217	18/02	670	164	537	103	181
CTD-009	-66.893	119.418	20/02	1080	1162	1952	613	534
CTD-010	-66.185	120.504	21/02	530	254	592	117	142
CTD-012	-66.388	119.749	25/02	650	433	1433	234	510
CTD-013	-66.485	120.333	25/02	600	592	2937	2230	1202
CTD-014	-66.506	120.487	06/03	490	166	455	194	155
CTD-015	-66.129	120.464	06/03	560	187	905	158	846

Sample ID	Latitude	Longitude	Collection Date (2014)	Water depth (m)	IPSO ₂₅ (ng g ⁻¹)	HBI III (ng g ⁻¹)	IPSO ₂₅ /HBI III	Epi-brassicasterol (ng g ⁻¹)	24-Methylencholesterol (ng g ⁻¹)	22-Dehydrocholesterol (ng g ⁻¹)	Cholesterol (ng g ⁻¹)	22-dihydrocondrillasterol (ng g ⁻¹)
sediments * (1-2 cm)												
MC-45	-66.398	120.589	26/02	538	34.5	3.1	11.3	1272	LOD	981	1881	LOQ
MC-61	-66.128	120.464	05/03	579	45.1	6.0	7.5	957	LOD	458	688	LOQ

LOD-below detection limit

LOQ-present, at the level of quantification

*No fatty acids measured for sediment samples